Suitability of two sensor technologies to monitor spatio-temporal patterns of soil moisture on extensive green roofs

Auteur : Bernard, Cédric
Promoteur(s) : Garré, Sarah
Faculté : Gembloux Agro-Bio Tech (GxABT)
Diplôme : Master en bioingénieur : sciences et technologies de l'environnement, à finalité spécialisée
Année académique : 2017-2018
URI/URL : http://hdl.handle.net/2268.2/5181

LIÈGE université
Gembloux
Agro-Bio Tech

Suitability of two sensor technologies to monitor spatio-temporal patterns of soil moisture on extensive green roofs

Cédric Bernard

travail de fin d'études presenté en vue de l'obtention du diplôme de master bioingénieur en sciences et technologies de l'environnement

Academic Year 2017-2018

Supervisor:

Pr. Sarah Garré (ULiège)

LIÈGE université
Gembloux
Agro-Bio Tech

Suitability of two sensor technologies to monitor spatio-temporal patterns of soil moisture on extensive green roofs

Cédric Bernard

travail de fin d'études presenté en vue de l'obtention du diplôme de master bioingénieur en sciences et technologies de l'environnement

Academic Year 2017-2018

Supervisor:

Pr. Sarah Garré (ULiège)

"Anyone who believes in indefinite growth on a finite planet is either mad, fool, or an economist"
David Attenborough

Acknowledgements

First of all, I would like to thank my supervisor Pr. Sarah Garré, who offered me the opportunity to study this subject, for her help on my interrogations and her assistance through the process of this Master's thesis, but also for her kindness and motivation.

I would like to thank Sid, Simon, Elodie and Sam who helped me with the correction of my work.

Special thanks to Romain for his help in the script for the image segmentation and Jérôme for his assistance and tools for the roof installation.

Warm thanks to Chistophe for his huge help on the construction of the data-logger, the roof installation and the different debugging we had to face.

Thanks to the 'Garré's squad' composed of Thibault, Fif and Guillaume. They were my office partners and the coffee break were better with them!

Finally, thanks to Léa, my family and friends who supported me throughout this period.

Abstract

Green roofs have the ability to mitigate stormwater runoff and to reintegrate wild-life and biodiversity in urban areas. However, they constitute complex ecosystems that still encompass grey areas. For instance, there has been only few research conducted on the accuracy of sensors such as capacitive EC-5 or thermic PlantCare, given the specific composition of green roofs substrates. In addition, green roofs often present spatial heterogeneity such as differences in substrate depths or partially shaded areas. This heterogeneity is expected to impact Substrate Water Content (SWC) and consequently plants development. Hence, the objectives of this thesis was to test both types of sensors in green roof substrate and to monitor - with abiotic parameters and vegetation coverage - two plots on an extensive green roofs with two different depth and shadowed areas. Firstly, PlantCare appeared as the most suitable sensor for green roofs application, given EC-5 dysfunctions due to poor contact between the sensors and the substrate. Secondly, the difference in depth has an influence in SWC, since the deepest plots presented a higher SWC during the entire experiment. As a consequence, a disparity in vegetation coverage was noticed, as the deepest plot presented more than 20% of plant coverage while its neighbour had only 5%. Finally, the shadowed area presented a higher coverage of plants than the rest of the plot. However, the behaviour of SWC was more complicated to seize at this scale due to the presence of plants and the small volume of influence of Plantcare.

Résumé

Les toitures végétalisées diminuent le ruissellement des eaux de pluie et réintroduisent la biodiversité dans l'environnement urbain. Cependant, ce sont des écosystèmes complexes dont les connaissances sont encore lacunaires. Par exemple, les capteurs de teneur en eau comme l'EC-5 ou le PlantCare ont été assez peu étudiés dans des substrats de toitures, substrats présentant cependant une composition qui peut altérer l'efficience des mesures. De plus, les toits verts présentent souvent des hétérogénéités spatiales, comme une différence de profondeur de substrat ou un jeu d'ombrage. Ces hétérogénéités impactent la teneur en eau qui contrôle le développement végétal. L'objectif de ce travail a dès lors été de tester les capteurs sur un substrat de toitures vertes et de suivre les paramètres abiotiques et le développement végétal de deux parcelles d'une toiture extensive avec des profondeurs différentes et un jeu d'ombrage. Le PlantCare a d'abord été élu comme le plus adapté, étant donné la difficulté de l'EC-5 d'établir un bon contact avec le substrat. Ensuite, la différence de profondeur influence l'évolution de la teneur en eau, celle-ci étant grande pour la parcelle la plus profonde. Cela a induit un développement inégal de la végétation entre les parcelles, avec plus de 20% de couverture chez la parcelle la plus profonde et seulement 5 % pour l'autre. Enfin, la partie ombragée a présenté un développement végétal plus important. Néanmoins, l'évolution de la teneur en eau est plus difficile à capter à cette échelle à cause de la présence de végétation et la localité des mesures.

Contents

List of Figures

List of Tables

Glossary

ANN Artificial Neural Network. 37

EM Electromagnetic. 32

ET0 Reference EvapoTranspiration. 19

FAO Food and Agriculture Organization. 20

FC Field Capacity. 6

FDR Frequency Domain Reflectometry. 32

IRM Institut Royal de Météorologie / Royal Meteorological Insitute. 15

PWP Permanent Wilting Point. 6

SWC Substrate Water Content. iii

TDR Time Domain Reflectometry. 32

USDA U.S. Department of Agriculture. 6

Foreword

This master thesis was partly written in the form of a scientific paper. Indeed, this structure allows the construction of a document that is clear and succinct.

The document is structured as follows the first part is written as a scientific paper. The second part includes an in-depth state of the art of the knowledge required to write this paper, and some additional informations about the experiment.

Part I

ARTICLE

1 Introduction

Nowadays, there are 7.6 billion humans living on Earth (U.N., 2017) and this number grows by 83 million every year. As a matter of fact, the world population will peak to 8.6 billion in 2030 and 11.2 billion in 2100, and can be considered in many aspects as a threat to the environment. For instance, if the population grows by 1 percent, the carbone dioxyde emissions are expected to increase by 1 percent (Jiang and Hardee, 2011). Yet, the world population is not only growing, it is also concentrating into cities, where 54% of human beings live today (U.N., 2014). This is called urbanization.

On the one hand, cities represent a promise of jobs and prosperity. They are a place for social and economic development, interconnections, culture and exchange of ideas. Through economies of scale, proximity and better infrastructures, cities reduce unit costs of different services such as electricity, public transport, health care or rubbish collection (Satterthwaite, 2000). Moreover, Dodman (2009) showed that per capita emissions of most cities are lower than their respective national average.

On the other hand, urbanization leads to substantial changes in the permeability of soils (Castiglia Feitosa and Wilkinson, 2016). Indeed, cities are mainly built using impervious materials such as concrete, glass, metal or tarmac (Scalenghe and Ajmone-Marsan, 2009). This sealing results in a decrease of groundwater refill and a significant increase of rainwater runoff, which leads to a higher risk of floods. In addition, cities centres generally lack green areas. This induces a loss of biodiversity and degrades human health and happiness (Berry and Okulicz-Kozaryn, 2011; Turner et al., 2004).

Solutions to mitigate negative impacts of urbanization are various. Among others, green roofs are becoming popular. Indeed, roofs constitute 20-25% of urban surfaces and they constitute big horizontal areas that are mostly unused (Susca et al., 2011). When vegetated, roofs have interesting properties. Firstly, they intercept and absorb rainfall, resulting in a decrease of runoff and an increase of runoff water quality ; which provides a solution against floods (Mentens et al., 2006). This problematic was studied at two differents scales : roof and city/regional scale. At roof scale, Zhang et al. (2015) showed that green roofs retain in average 77.2 % of stormwater runoff and Berndtsson et al. (2009) proved that green roof increase runoff water quality. At city/regional scale, Carter and Jackson (2007) discovered the high potential of rooftops as stormwater runoff management at watershed scale. Moreover, a conceptual hydrological model was developed by Versini et al. (2015) at a basin scale and they observed that green roofs have a significant impact on urban runoff in terms of peak discharge and volume.

A second interesting property is the ability of vegetated roof to provide shelters for biodiversity. Concerning fauna, Colla et al. (2009) showed that green roofs constitute suitable habitat for foraging and nesting of bees, and Fernandez-Canero and Gonzalez-Redondo (2010) as habitat for birds. Concerning flora, Madre et al. (2014) presented green roofs as new spaces for wild plants establishment. However, one of the biggest challenges for researchers reside in developing mixes of plants that are suitable for green roofs. As explained by Francis and Lorimer (2011), the ecological functions of green roofs will be maximize via varied and heterogeneous designs (e.g. substrate depth, substrate composition or spatial structures) and varied composition of plants.

The purpose of this study is to examine the potential of extensive green roofs to retain rainfall and keep water available for plants in its substrate, but also to enhance biodiversity in cities by creating new 'habitat analogues'. More specifically, we (i) investigated which sensor technology is suited to quantify moisture content in extensive green roof substrate, (ii) used these sensors to monitor water content in space and time on two green roof plots with different substrate depths, and (iii) studied to which extent species of meso-xeric grasslands were able to develop under the conditions met in these green roof plots.

2 Material & Methods

2.1 Experimental site

The experimental site is located in Gembloux, Namur, Belgium (50°33'48.3"N,4°41'53.3"E). The green roofs are located on the roof of TERRA Teaching and Research Centre, which is a new building in the main street of Gembloux, Avenue de la Faculté.

Figure 1: *Location of Gembloux in Belgium.*

Figure 2 presents a sky view of the studied roof. Plots A and B are not considered in the scope of this thesis, as we focused on plots C exclusively. Due to the limited number of sensors and the side effects resulting from small areas of plots C2, C3, C4, C6, C7, C8, C9 and C10, only plots C1 and C5 were studied.

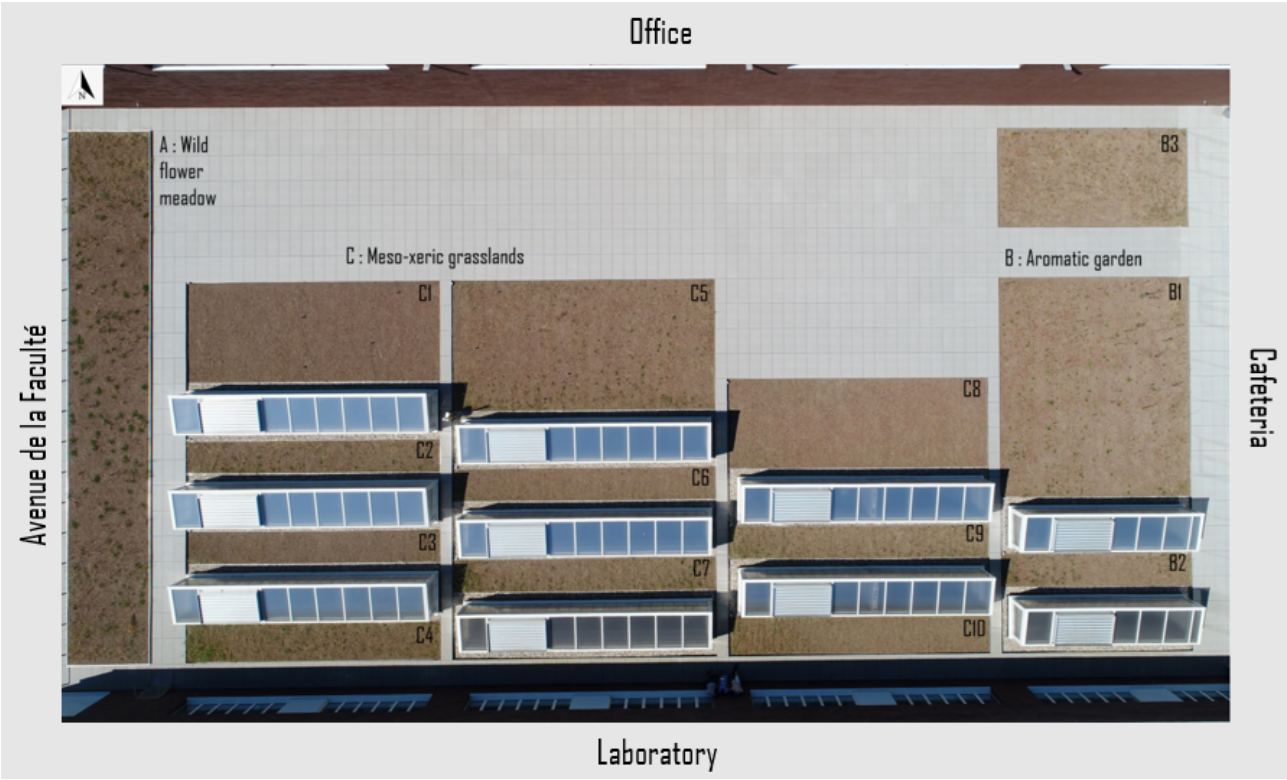

Figure 2: *Sky view of the experimental green roof of TERRA, with the studied plots C1 (8cm deep) and C5 (14cm deep).*

Plots differ from each other in terms of surface ($45m^2$ for C1 and $61m^2$ for C5) and substrate depths. The experimental green roofs are extensive ones, with C5 being the deepest plot (with initial depth of 14 centimetres, while C1 is 8 centimetres deep). The substrate was not compacted before its establishment: therefore a natural compaction must occur, by 20 % of the initial volume following Zinco datasheet (Appendix 1). The measurements of depths resulted in an average of 12.9 ± 0.7 and 7.2 ± 1.3 centimetres, respectively for C5 and C1.

2.2 Substrate

For this experiment, the commercial substrate 'Rockery Type Plants-Light' from Zinco was used. This substrate is composed of a mix of crushed brick, mineral aggregates, substrate compost and fibre materials. On the picture (Appendix 1), we can notice the heterogeneous composition of the substrate. Indeed, there are areas with a lot of fine matter and areas that are concentrated in mineral aggregates. Consequently, water will not be equally distributed in this heterogeneous composition, which will introduce some complications in the measurements.

Pressure plates experiment was achieved to get suction - θ_v relationship for this substrate. A retention curve was then fitted using Van Genuchten model, which is presented hereunder (Figure 3). Three parameters of the substrate were obtained: θ_s, the volumetric content at saturation, is 0.29. Alpha (α), inversely proportional to mean pore diameter, is 0.27. Finally, n, the shape parameter of soil water characteristic, is 1.15. The fraction of available water, obtained by subtraction of Field Capacity (FC) by Permanent Wilting Point (PWP), is equal to 0.08. The R^2, which represents the goodness of fit, equals 0.9927: this indicates qualitative regression of observed versus fitted values.

Based on the comparison of data from Yang and You (2013) and from the U.S. Department of Agriculture (USDA), we found that θ_s of our substrate is smaller than every other soil texture, thus it will reach saturation quicker. The α parameter is greater than every other soil texture, indeed a significant part of the substrate is constituted by big aggregates. Finally, the available water capacity is also very small, with typical values of sands smaller than 0.10.

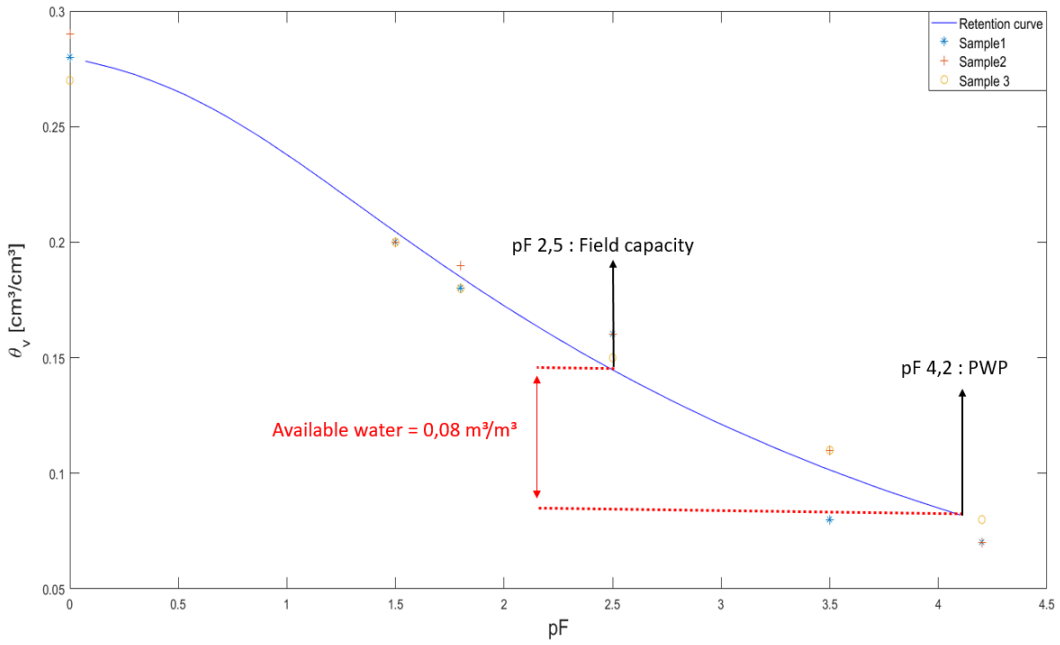

Figure 3: *Retention curve from pressure plates experiment fitted with Van Genuchten model.*

2.3 Sensors' calibrations

In the experiment, two soil water content sensors were used. The first one, based on capacitive technology, is the EC-5 from Decagon Devices. The second is the OEM Soil Moisture Sensor from PlantCare. This sensor is based on micro-thermic technology. Basically, a tip is enclosed in a hydrophilic felt is heated, the felt acting as an accumulation body for the water and is in equilibrium with the substrate. The cooling-down time of the tip is then related to SWC .

A classic calibration was performed under laboratory conditions and stable temperature, using protocol from Application Note of Decagon Devices (Cobos and Chambers, 2005). For PlantCare sensors, 3 plastic cylinders (2 of 11 cm of diameter and 20 cm of height, one of 10 cm of diameter and 20 cm of height) were used and, for EC-5, a cylinder of 30 cm of diameter and 25 cm of height was used. In order to best match field conditions, 8 cm of substrate were added to the cylinders. Substrate was oven-dried at $60°C$ for 48H. Starting from this state ($\theta_v = 0\ cm^3/cm^3$), water was added by steps of $\Delta\theta = 0.05\ cm^3/cm^3$ to reach saturation. SWC at saturation was obtained by previous saturation for retention curves and was $0.30\ cm^3/cm^3$. To achieve homogeneous distribution of the added water, substrate was hand-mixed at each step for several minutes and then the sensors were placed into it (Kargas et al., 2013). The felt of PlantCare sensors needs to equilibrate with the substrate (Matile et al., 2013), meaning that the measurements are correct in our case maximum 4 hours after the addition of water (see Figure 4). The water was added at 5 PM and the equilibrium is obtained around 10 PM. In the contrary, measurements for EC-5 could be achieved almost instantly. For both sensors types, 8 sensors were tested.

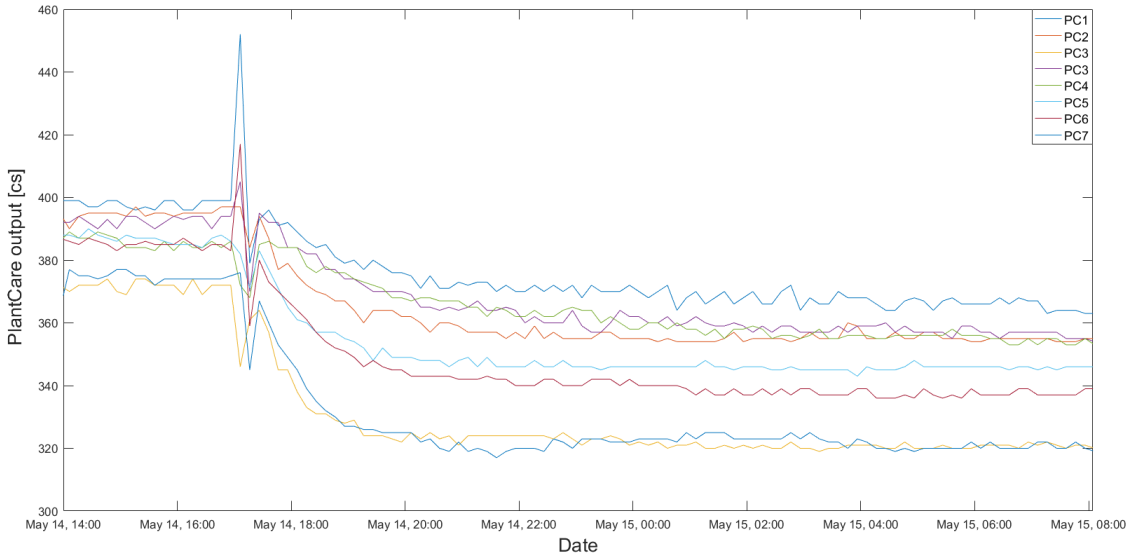

Figure 4: *Equilibrium time needed for correct measurement of PlantCare sensors after the addition of water.*

2.4 Experiment setup and measurements

Both studied plots are composed of the same mix of plants, which is a selection of 29 plants sowed on the 5th of October 2017. It consists in 4 gramineous species sowed at a density of 830 seeds per m^2, while the remaining plants were sowed at a density of 110 seeds per m^2 (among which 3 sedum species). The complete list of species is presented in the Appendix 2.

Those species were selected following the concept of analogous habitats. This concept establishes that urbanized sites can be colonized by plants that grow on analogue natural habitats. This is due to the conditions of the anthropological site, which are close enough to the ones of the natural site and present similar stresses that go along with these environments (Lundholm and Richardson, 2010). The mix of plants was then inspired by dry meso-xeric grasslands. These grasslands are growing on rockery and dry to very-dry substrates. Indeed, the plots of our extensive vegetated roof are confronted to conditions and constraints similar to the ones of these ecosystems (Lundholm, 2006), such as shallow depth of substrate, high drainage, dry conditions and high exposition to climate conditions.

The plants analysed in the two studied plots were sown by hand, which induces an inherent heterogeneity in this sowing. Ventilation and air extraction structures (2 m high) were built on the roof, creating differences in radiation along the plots. This expected gradient should have an influence of evapo-transpiration, having itself an impact on soil moisture: such a gradient should thus not be ignored. We modelled it using Sketchup Pro toolbox 'De Luminae Sun Ex-

posure'. The shade produced by the structures results in a radiation gradient along the width of the plots.

The following setup was therefore chosen to respect, on the one hand, the random distribution for sowing heterogeneity, and the gradient of shadowing on the other.

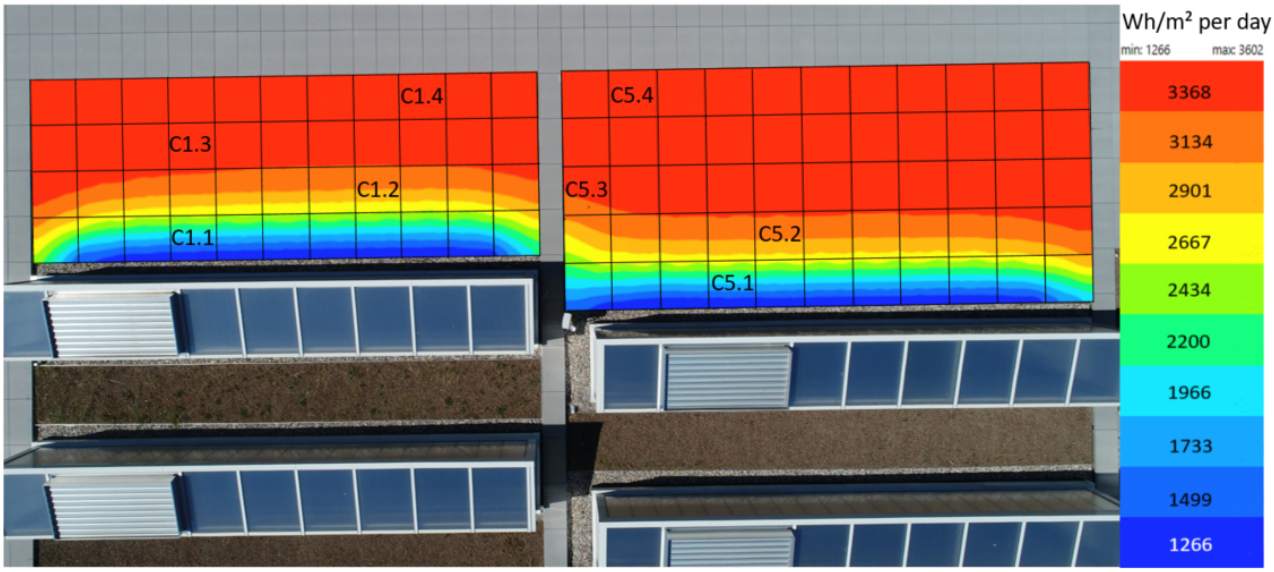

Figure 5: *Position of the quadrats equipped with sensors on the studied plots in function of the modelling of radiation gradient.*

In the frame of this experiment, 8 quadrats were defined. 4 are distributed along the width following the radiation gradient on each plot . In each quadrat, we can find one of each types of moisture sensors (EC-5 and PlantCare) and a radiation sensor (SP-100 from Apogee Light). Data were sampled from the 22nd of May 2018 to the 23rd of July 2018 and analysed using principally MATLAB software. Substrate water content was measured every 30 minutes by both sensors. For radiation, data were collected every 5 minutes. To measure the general conditions of the roof (i.e. air temperature, radiation, precipitation and wind), the micro-meteorological station ATMOS41 from Decagon Devices was used. This station was placed on a 2 meters high structure, so as to avoid any obstacles in the measurements. The period of measurements presented extraordinary values of air temperature and precipitations, a summer drought occurred with an intensity that was not observed since 1976 in Belgium.

To measure the development of plants on the plots, two different methodologies were developed. First, drone pictures of both plots were taken on 29th June. To quantify the vegetation coverage from these images, a segmentation, based on neural network, was computed. The second methodology was developed by Julie Reniers and is based on the point-quadrat method. Those methodologies are fully explained in the second part of this document.

3 Results & Discussion

3.1 Calibrations

The first objective of this thesis was to evaluate the two soil moisture sensors in their ability to seize SWC in Zinco substrate.

Results from EC-5 Calibration are presented in Figure 6. There are 8 outputs for each step of SWC, since there are 8 tested sensors. Moreover the mean value of the 8 outputs was computed and plotted as a plain black dot. Calibration curve resulting from this mean value was fitted using MATLAB Curve Fitting Tool, which allows to test multiple fitting curves and to obtain the goodness of fit.

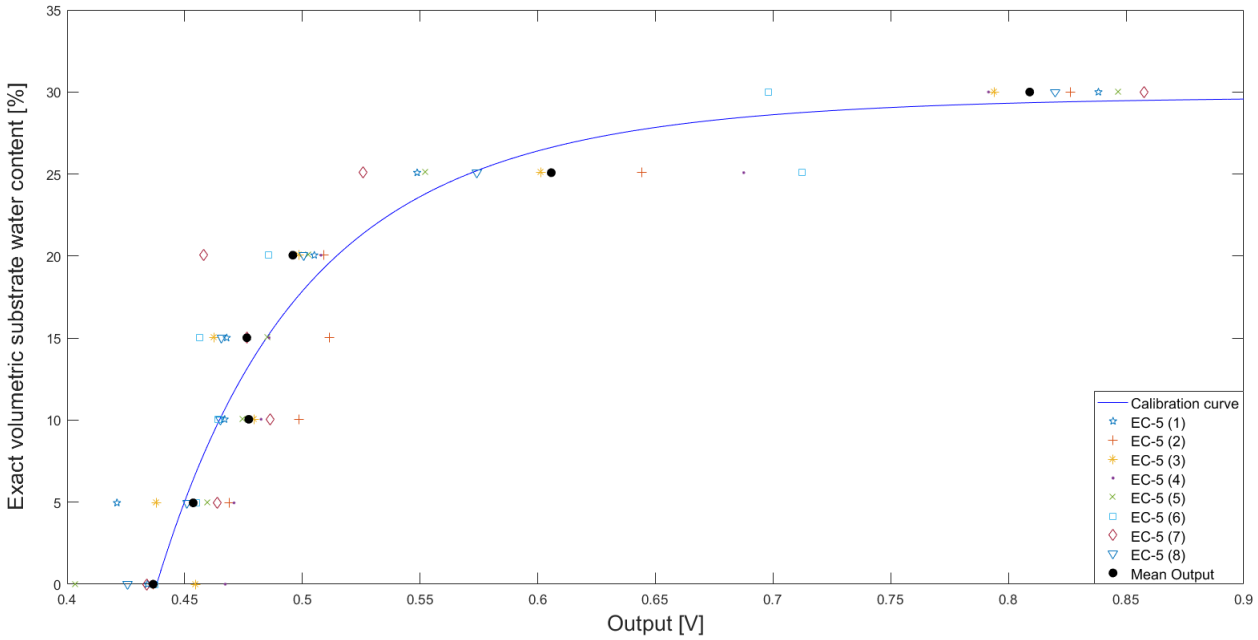

Figure 6: *Calibration curve for EC-5 sensors, with the 8 outputs (volt) by steps of SWC and the mean values as plain black dots.*

The calibration curve resulting from laboratory experiment has a logarithmic shape. Its equation is expressed as

$$y = 0.09751 * x^{-6.932} + 29.77 \tag{1}$$

with y representing SWC and x the EC-5 Output. The goodness of fit, expressed as R^2, is 0.9472. Based on the shape of the curve, we can reach one important conclusion: the EC-5 is less sensitive at water contents lower than 0.20 cm^3/cm^3 than it is at wetter ranges. When increasing SWC in those values, only a slight change in the EC-5 output range will be measured. This would not have importance consequences if the variation between sensors is low, every step would have a different output range. But this is not the case since variability between sensors is

great, and this is valid for every steps of SWC. This leads to a considerable issue: for instance, a voltage output of 0.46V can correspond to multiple substrate water contents: 0, 5, 15 and 20 %, and the calibration curve indicates 10 %. Based on this observation, we face a significant uncertainty in low voltage outputs, as we are unable to determine if a given output value corresponds to a certain volumetric substrate water content. In addition, the point of 0 % SWC does not correspond to a 0V output signal. This results in negative SWC values when voltages below the mean minimum point (0.43V) of the curve are converted. This conversion is therefore not physically possible: thus this constitutes another disadvantage for EC-5. These issues lead to a first conclusion: EC-5 sensors are not suitable for low SWC in Zinco rockery-type substrate.

This issue in low SWC can be explained by the fact that capacitance probes such as EC-5 need to have perfect contact with soil matrix (Regalado et al., 2007). Hence, if no good contact can be assured, bias are expected. Our substrate, made of mineral particles with organic matter added, is not homogeneous and will not allow perfect contact with the probes. Indeed, this kind of substrate produces air pockets without any trace of substrate, resulting in areas where the sensor is not in perfect contact with substrate matrix (Souto et al., 2008).

The calibration of PlantCare sensor is presented in Figure 7. The protocol to find the calibration curve is the same as for EC-5.

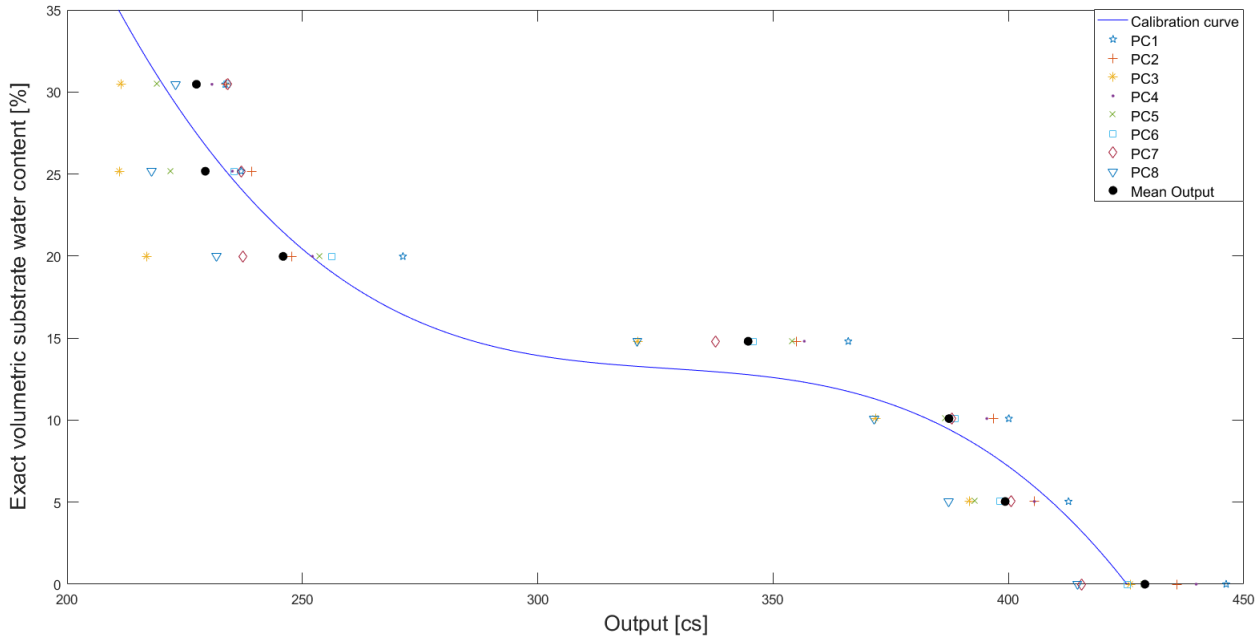

Figure 7: *Calibration curve for PlantCare OEM sensors, with the 8 outputs (centi-seconds) by steps of SWC and the mean value as plain black dots.*

Resulting calibration equation is a third degree polynomial equation and is presented hereunder:

$$y = -1.228 * 10^{-5} * x^3 + 0.01208 * x^2 - 3.98 * x + 452.3 \quad (2)$$

with y the SWC and x the time of cooling of PlantCare sensors. The R^2 of the fitting is 0.9649. This kind of curve was already encountered in another calibration of PlantCare sensors (Matile et al., 2013) and means that PlantCare sensors are very sensitive in 15-20 % water content. Indeed, a significant change in the ouputs in those values will introduce a slight change in SWC. From 0-10 %, the curve is steep but the variability between measurement is quite low, thus only few overlaps exist. From a range of 20 to 30 % SWC, the curve is also steep but the variability between measurements is much larger, resulting in some overlays of the data. The issue behind this variability will be discussed in the next paragraph. However, we can already notice that this error in higher SWC will not be dramatic in our application, since these SWC are not often found in green roofs substrate. This is due to the drought inherent with these ecosystems, which was worsened by the extremely dry summer during the measurements.

In order to compare the variability of measurements between sensors, the coefficient of variation was computed (Figure 8). Given the fact the sensors have different units, this coefficient was used since it is independent of units.

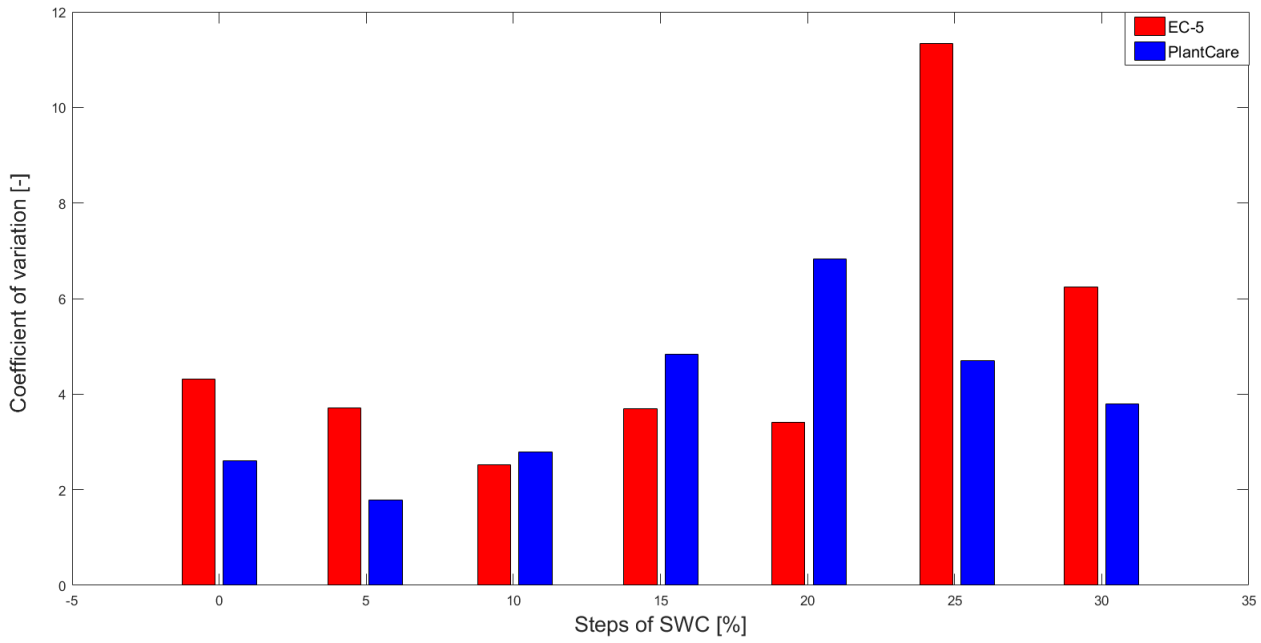

Figure 8: *Coefficient of variation of EC-5 VS PlantCare sensors for every steps of volumetric water content.*

This graph concludes our reflection on sensors. For EC-5, the variation of low and medium

SWC (0-20 %) is not particularly considerable. However, because of the steepness of the curve, the data overlap on other SWC steps. Hence, even if the variation is sometimes lower than PlantCare, no certitude can be drawn at these SWC by EC-5. For high SWC (25-30%), EC-5 sensors present a much higher variability than PlantCare and thus can not be used.

For PlantCare, the variability until 15% SWC is low, but increases from there and decreases at 25%. It can be explained by the fact that, at these water contents, a considerable heterogeneity in terms of humidity can be found in the substrate. Indeed, the fine matter will be very humid because it absorbs water first whereas bigger aggregates will be less humid. Moreover, PlantCare sensor makes very local and restricted measures, since all measurements are performed within a thin volume of substrate around the felt. This increase in variability can be explained by the environment of the sensors: if their felt is surrounded by a lot of fine matter, it will measure a high SWC, almost reaching saturation for some sensors. Thus, based on this reasoning, if the sensors is closer to mineral aggregates they will measure lower SWC.

Our main conclusion, based on these calibrations, is that PlantCare is the most suitable device for our application. Indeed, two main issues were put forward for EC-5 sensor. First, at low SWC, given the shape of the curve a lot of data overlap was observed. The second problem is the variability between sensors at high SWC: this variability is greater than with the use of PlantCare sensors. Therefore, for the rest of the measurements, only data from PlantCare sensors were thus purposefully used, while EC-5 were still set up in case of failure.

3.2 Effect of depth on the evolution of water content over time

The second objective of this thesis was to monitor the evolution of SWC in space and time on two green roof plots with different depths.

Previous studies showed that substrate depth is the major factor for water-holding capacity. Deeper substrate increases the amount of precipitation intercepted and accumulated (Getter and Rowe, 2006; Nardini et al., 2012). The way substrate depth impacts substrate water content over time was thus tested. For this purpose, we averaged the four sensors per plot and compared both plots in Figure 9. We also considered standard deviation of the sensors to ensure that differences between plots were not due to any uncertainty. This standard deviation is computed based on the calibration variability, thus this variability as STD is changing at every SWC step.

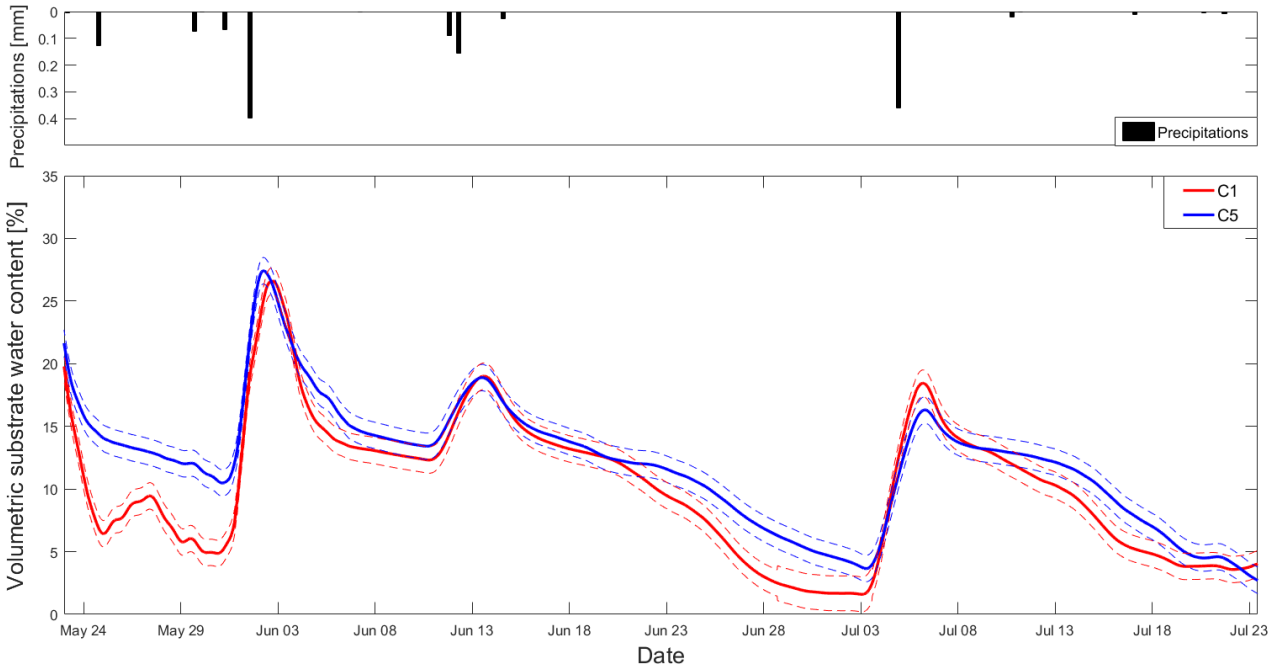

Figure 9: *Effect of substrate depth on SWC measured by PlantCare over time for the two plots with different depth: 8 centimetres (red, C1) and 14 centimetres (blue, C5).*

Several conclusions can be drawn from the graph on Figure 9. First, the deepest plot (C5) presented at all steps of the experiment a higher SWC than its shallower neighbour. However, the difference between both plots is changing during the experiment. Second, as shown in the upper part of Figure 9, several small rain events took place during the period of measurements. After every rain event, both plots reached the same SWC as already shown by Nardini et al. (2012), with an exception of the precipitation on the 4th of July where C1 seems to get slightly higher SWC. Third, the difference between plots lies in the drying rate after rain event, C1 presenting higher rates of drying than C5 after a certain time. For instance, on the precipitation of the 11th of June, both plots reached the same peak of SWC (around 20%). After that, they dried at the same rate until the 20th of June. From this date, C1 dried at a higher rate than C5, resulting in significantly lower SWC until the 3rd of July. This behaviour was expected, since shallower depths mean less heat inertia, resulting in hotter substrate (Nardini et al., 2012), more evaporation, less retention and detention of rainfall (Yio et al., 2013). Consequently, after a certain time following a rain, C1 is less efficient to keep the water available for plants than C5. This difference in water-holding capacity have an impact on vegetation development and diversity, since green roofs constitute extreme ecosystems where water availability is a major factor for plant development (Thuring et al., 2010; Nagase and Dunnett, 2010).

3.2.1 Impact on vegetation coverage

By looking at the drone pictures on the top of the Figure 10, vegetation on plot C1 is practically absent, while there is some vegetation well established on C5. This difference in vegetation is due to soil water content, since any other parameters that could influence the development of plants such as radiation, sowing density, precipitation, type of substate etc. (Haferkamp, 1988) remained the same during the experiment on both plots.

An issue we encountered with the segmentation resides in the dry gramineous that are laid down on the substrate and present by example on the top left of C5 plot. These herbs have a very similar color to some of the substrate aggregates. Thus, some aggregates were mistakenly segmented, resulting in an over-estimation of vegetation coverage. To counter that, we eliminated from the segmentation the round aggregates, which however resulted in some of the segmented dry gramineous being cut into small points. This leads to a slight underestimation of the coverage, because some gramineous are not fully segmented. This underestimation will be most important in the zone were the dry gramineous are massively present. However, the segmentation correctly follows the vegetation of the plots: a comparison between drone pictures and binarized pictures indicates that the algorithm could efficiently separate vegetation and substrate. The results of this segmentation show differences in vegetation coverage, as it was visually the case from the drone pictures. The results of this segmentation are presented in Table 1. In addition, the work of Julie Reniers is also presented (complete protocol in part II).

This table gives us more details about how the species react to the difference of depth and gives us a comparison with our segmentation. For C1, we can see that segmentation and coverage measurements are very close. For C5 however, a difference of 5 % exists between the two methods. On one hand, segmentation treats all the plot but the presence of dry grass leads to an underestimation in the zone where these grasses are massively present. On the other hand, the point-quadrat method only measure certain quadrats, thus does not cover all the plot. It was then interesting to have both methods to allow a comparison.

The species *Anthoxanthum Odoratum L., Anthyllis Vulneraria L., Koeleria Macrantha (Ledeb.) Schult,* and *Medicago Lupulina L.* are significantly affected by the factor depth, but we can also notify that species coverage is always greater in C5 than in C1, indicating that the deepest plot is more suitable for the development of meso-xeric grasslands. Indeed, deeper substrate can ease the development of plants because of better conditions. For instance, temperature range are lower (Nardini et al., 2012), it dries slower as it was shown by our measurements and by Chenot et al. (2017), but also plants as *K. Macrantha* can extend its roots deeper to avoid water deficit (Mueller-Dombois and Sims, 1966).

Table 1: *Response in terms of vegetation coverage to the difference of substrate depth of the different species of meso-xeric grasslands in both plots, with their corresponding p-value (in bold when significantly different between the two modalities and with * when the homogeneity of the variances are not respected).*

	Depth [cm]		
	6	12	
Species	Coverage [%]		p-value
A. odoratum	3.3 ± 2.4	10.4 ± 4.6	**0.0063**
A. vulneraria	1.3 ± 2.3	4.1 ± 2.8	**0.0001**
B. media	0 ± 0	0.2 ± 0.6	0.1529
B. erectus	0.6 ± 1.1	2.4 ± 1.8	0.517
D. carota	0 ± 0	0.2 ± 0.4	0.3051
E. vulgare	0 ± 0	1 ± 1.1	0.0625
K. macrantha	0.7 ± 0.8	5.4 ± 2.9	**0.005***
L. corniculatus	0 ± 0	0.7 ± 0.8	0.088
M. lupulina	0.3 ± 0.8	2.3 ± 1.8	**0.0073**
P. pratensis	0 ± 0	0.1 ± 0.3	0.484
S. columbaria	0 ± 0	0.3 ± 0.7	0.08
S. vulgaris	0 ± 0	0.3 ± 0.5	0.1912
T. pratensis	0 ± 0	0.2 ± 0.4	0.1499
S. acre	0.1 ± 0.4	0 ± 0	0.2946
C. album	0 ± 0	0.1 ± 0.3	0.2946
Total	6.3	27.7	
Segmentation	5.51	22.72	

However, it is important to cautiously consider these results. Along the period of measurements appeared extraordinary weather conditions in terms of air temperature and precipitations, this period of measurements occurring during a summer drought. Indeed, precipitation measurements indicate that only 1.35 mm of water fell on the plots, which was not seen in Belgium since the drought of 1976, a record year. However, the Institut Royal de Météorologie / Royal Meteorological Insitute (IRM) measured 30 mm of precipitation for our measurement period, the precipitations on the plots being thus well under the national average. Two explanations are possible: Gembloux was particularly impacted by the drought or the configuration of the building did not allow all the rainfall to reach the plots. Thus the conclusions we draw considering the vegetation development on the two plots are valid for our measurement period, but to have a long-term behaviour between the two plots this experiment should be lead for few more years.

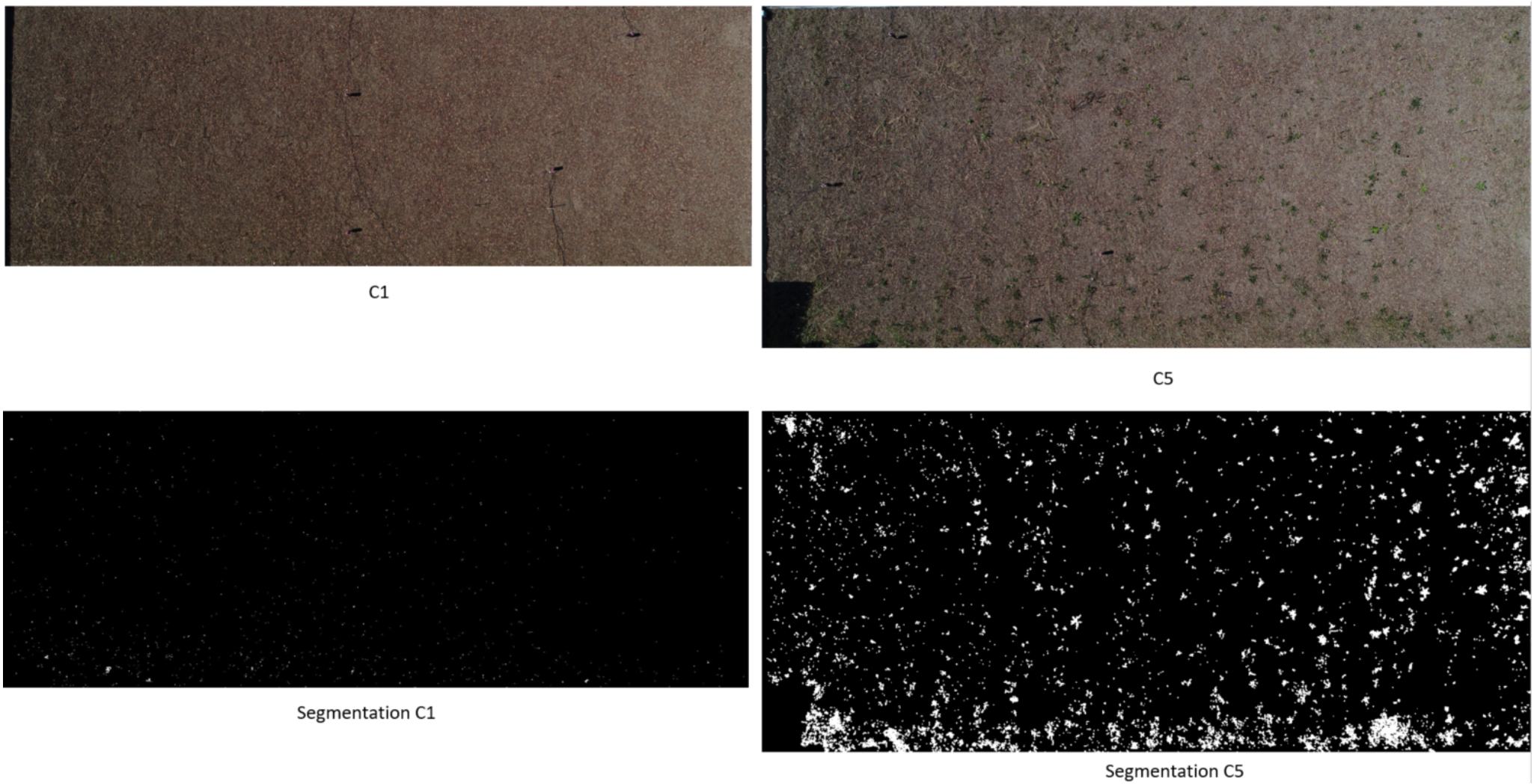

Figure 10: *Top: Drone picture of plots C1 on the left and C5 on the right ; Bottom: corresponding segmentation by neural network from the drone pictures.*

3.3 Variability within plot C5

The following section aims to fulfil our last objective: how the mix of plants and SWC are affected by the spatial variability on the roof. For this purpose, we only focused on plot C5, since the other plot faced very small plant development.

If we look closely to plot C5 in Figure 10, we can notice differences in terms of vegetation coverage between the quadrat that is closer to ventilation structures and the rest of the plot, as shown by the Figure 11. To construct this graph, we split the width of the plot in 20 equal parts, and calculated the coverage percentage in each small subplot from the segmented image.

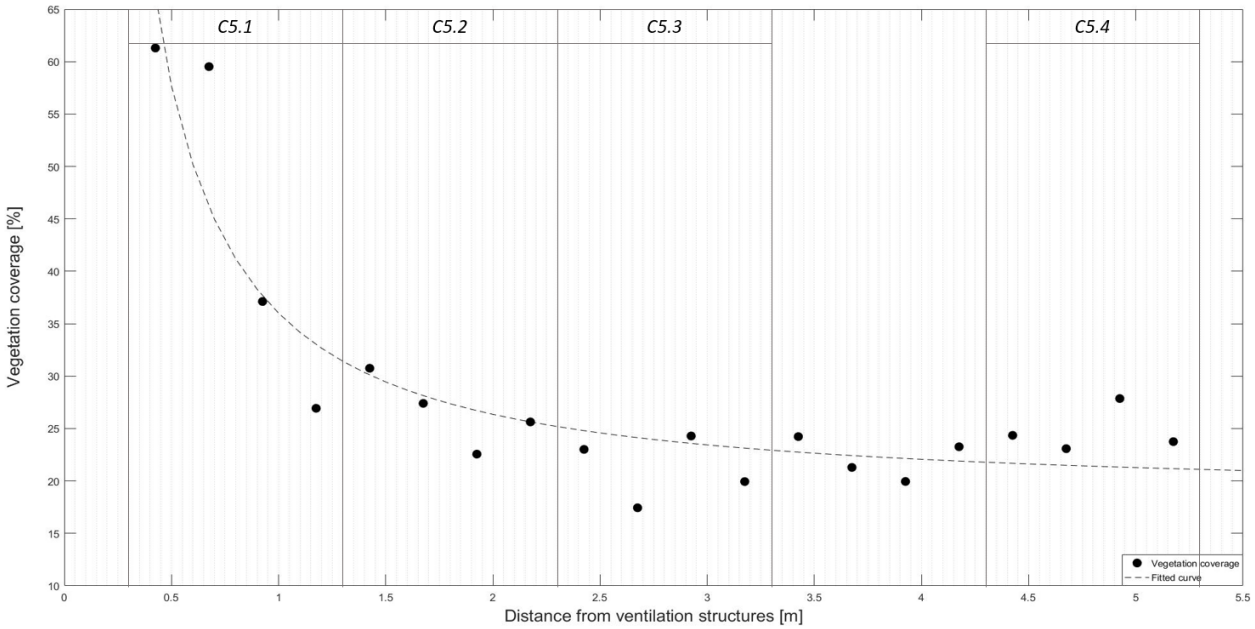

Figure 11: *Evolution of vegetation coverage percentages on plot C5 in function of the distance from ventilation structures.*

We can notice that the percentage of coverage decreases when the distance from ventilation structures increases. A plateau is achieved starting from 1.5m, thus we can hypothesize that conditions for plants are better in the width containing C5.1 than for the rest of the plot. On the plot C5, the parameter that can influence plants development (e.g. the type of substrate and thus nutrients, rain events, air temperature, air composition, relative humidity, wind, sowing density) are supposed to be all the same on the plot (Haferkamp, 1988). The only element that may vary within the plot is the radiation, because of the spatial environmental heterogeneity created by ventilation structures (Buckland-Nicks et al., 2016). This radiation gradient is then supposed to be the main principle responsible for this vegetation heterogeneity. We will therefore describe this gradient and its consequences on both abiotic parameters and vegetation.

3.3.1 Spatial heterogeneity of abiotic parameters in C5

Figure 12a presents the evolution of radiation through a typical day and confirms partially the modelling from SketchUp pro (Figure 5). The reference is always above the quadrats, thus a shadow evolution on the plot is definitely present. C5.1 presents much smaller radiation than all other quadrats, as it was shown by the model. In addition, measurements show that this lack of radiation begins at 7AM and ends at 14 PM, when sunshine starts to hit ventilations from South. Modelling presented a gradient of increasing radiation starting from C5.1 to C5.4. On the contrary, the measurements show that the second quadrat that receives less radiation is C5.4, which is the furthest quadrat from ventilation. This phenomenon raises our astonishment since no shadow was observed on this quadrat. However, we can notice that the difference between the three quadrats is very small.

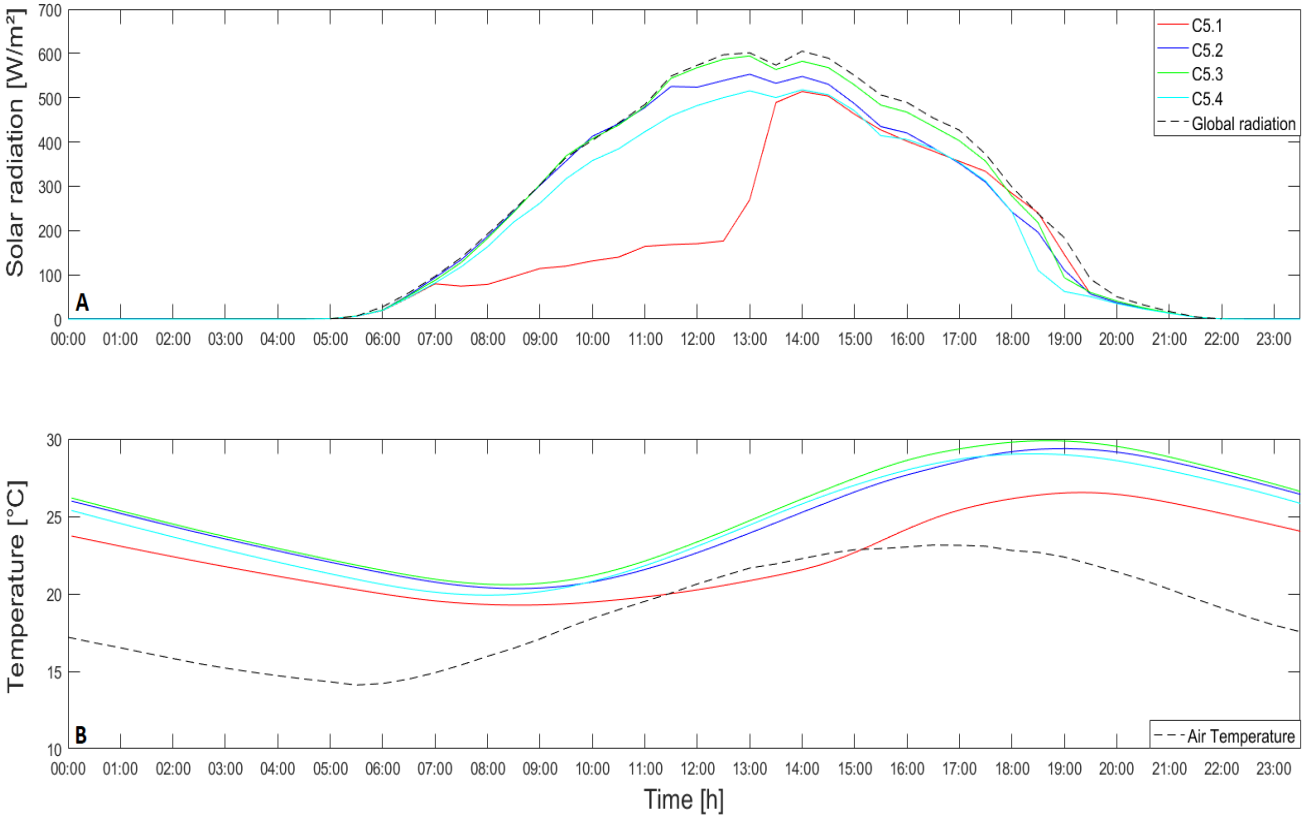

Figure 12: *(a): mean daily evolution of solar radiation [W/m^2] of the four quadrats of C5 and the reference radiation from micro-meteorological station (dotted line) ; (b) mean daily evolution of substrate temperature by quadrat (°C) and the air temperature (dotted line).*

This gradient in radiation will have multiple and complex consequences on the development of plants. Indeed, when plants develop in unstressed conditions, an increase of sun exposition leads to a increase in plant growth (Beaudet and Messier, 1998). However, as mentionned before, on the one hand green roofs constitute extreme ecosystems and, on the other hand, the

period of measurements occurred during a period with almost no precipitations. Plants were then growing under stress due to water scarcity. This leads the increase of radiation to have more bad effects: augmentation of substrate temperature, evaporation, etc.

The first consequence radiation gradient has is on substrate temperature. This temperature follows the course of air temperature due to the evolution of the day, but radiation implements differences between quadrats, as shown in Figure 12b. C5.1, receiving less radiation during the day, presents the lowest substrate temperature. This difference becomes the highest starting at 10AM, when this quadrat stays under the shadow, while the others get warmed up by sunshine. This difference is maintained after radiation differences stop (14PM), because of the inertia of the substrate. Thus the solar differences will have consistent consequences on substrate temperature during all day. The slight differences observed in terms of radiation between C5.2, C5.3 and C5.4 in Figure 12a do not reflect on substrate temperature, since the one that receives the most radiation (C5.2) has the coolest substrate temperature, even if the differences are small.

The differences in substrate temperature that were put forward hereabove can have repercussions on the abiotic conditions of the quadrat. Increase substrate temperature will induce increased evaporation (Monteith, 1965), thus provoking a diminution of SWC. A similar spatial heterogeneity of shadow has already been studied, the difference of shadowing resulting in a difference of substrate temperature and SWC driven by this gradient (Buckland-Nicks et al., 2016). Getter et al. (2009) also showed that SWC was higher in the shade area than in the sun within the same substrate depth. We continue our analysis by focusing on the effect of the differences in radiation and substrate temperature on Reference EvapoTranspiration (ET0) in Figure 13

The ET0 was computed using ET0 Calculator from the Food and Agriculture Organization (FAO) (Raes, 2009). This parameter allows us to study the soil evaporation and reference crop (grass) transpiration. This is a meteorological parameter since variability from crop type, field practices and crop development are not taken into account. In our case, the loss of water will predominantly be caused by soil evaporation. Indeed, as the surface is not well covered by plants, the transpiration cannot be the main process (Zotarelli and Dukes, 2010). For the computation, the equation from the FAO Penman-Monteith is used, with influencing parameters being the air temperature (maximum, minimum and mean values in °C), the mean relative humidity of air (%), the mean wind speed (m/s) and the solar radiation (MJ/m^2.day). The latter parameter being the only one that changes between quadrats, this is the solar radiation that will explain possible differences in ET0.

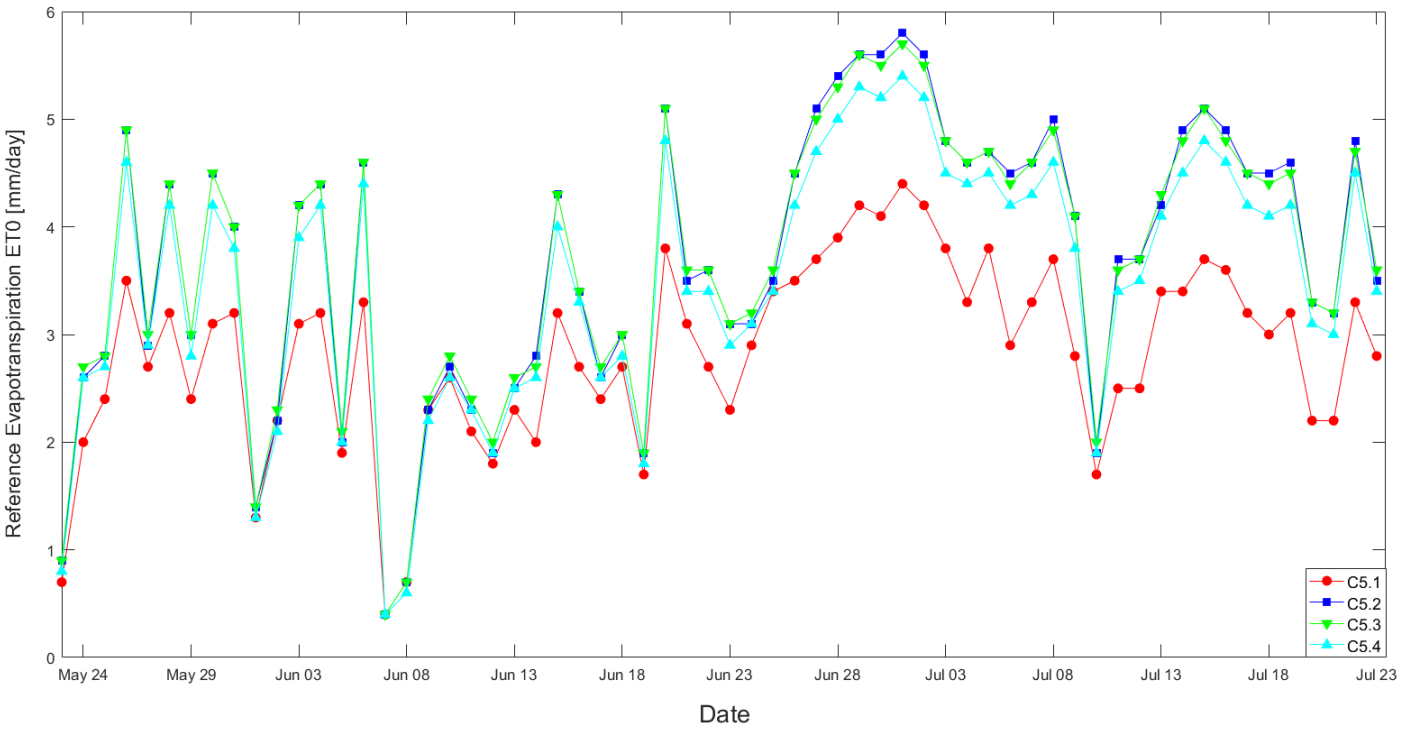

Figure 13: *Reference evapotranspiration (ET0) evolution over time of the four quadrats of C5.*

Figure 13 shows, as expected from the previous parameters, that C5.1 presents lower ET0 rates for the whole experiment than the three others, the latter ones presenting very similar rates. The parameter ET0 expresses the evaporating power of the atmosphere at a specific location (Allen et al., 1998), thus a lower ET0 (like C5.1) means that this quadrat is supposed to have less ability to lose water (in terms of climate) than the others. The differences in evapotranspiration should then have an impact on the SWC and create a gradient of SWC.

3.3.2 Impact on vegetation coverage

The following table gives a more detailed information of the difference in terms of vegetation the difference in radiation created on the plot C5. Again the values by species come from the work of Julie Reniers. From the segmentation, we see that C5.1 presents the higher coverage and the three others plots presents smaller coverage. The measurements of plants coverage and the segmentation results are very close from each other, for both high radiation and the plot with shadow, which indicates that segmentation and point-quadrat method correspond even at the scale of the quadrat.

Table 2: *Response in terms of vegetation coverage to the difference in radiation on plot C5 of the different species of meso-xeric grasslands, with their corresponding p-value (in bold when significantly different between the two modalities and with * when the homogeneity of the variances are not respected).*

	Plots		
	C5.1	C5.2, C5.3 & C5.4	
Species	Coverage [%]		p-value
A. odoratum	10 ± 2.8	7.7 ± 7.8	0.582
B. erectus	2.5 ± 2.1	1.2 ± 1.8	0.33
K. macrantha	5.5 ± 6.4	2.8 ± 3.2	**0.0161***
A. vulneraria	5.5 ± 6.4	1.3 ± 2.2	**0.046**
E. vulgare	0	0.8 ± 1	0.067
L. corniculatus	0	0.3 ± 0.5	0.347
M. lupulina	4 ± 2.8	0.8 ± 1.6	0.058
P. pratensis	0	0.2 ± 0.4	0.643
S. vulgaris	0	0.2 ± 0.4	0.643
Total	27.5	15.3	
Segmentation	32.13	17.2	

C5.1 presents a total coverage of 27.5% from coverage measurement and 32.13 % from segmentation. The dominant species are the gramineous, as it is the case in the other quadrats. This higher coverage is due to the conditions present on this quadrat, such as the presence of shadow. For the three other plots, abiotic parameters led to a similar plant development, as seen with the segmentation (17.2 %) and with the point-quadrat measurements (15.3 %). Two plants were significantly more present in the lower exposed quadrat: *A. vulneraria* and *K. macrantha*. The higher coverage means that the presence of shadowed area, in the particular environment of green roofs under dry summer, created better condition for plant development.

3.3.3 Impact on SWC

Figure 14 shows the evolution of the four quadrats of C5 in terms of SWC during the experiment. Until the 23th of June measurements all stayed in a close range. Moreover, we can notice that the same order is respected, in increasing order of SWC: C5.4, C5.3, C5.1, and finally C5.2. From the 23rd of June to the rain event of the 5th of July, the differences between sensors become much larger. C5.4 is practically at 0% at the end of the month of June but C5.2 stays above 10%. After the rain event, the substrate is drying but, from the 14th of July, C5.3 goes up again with no precipitations registered, which is not an expected behaviour. The second part of the figure shows a zoom on the 23rd of July when the sensors were put out of

the substrate. To have a direct and precise measurement of substrate moisture at this time, we sampled substrate at every PlantCare sensor location and used the thermo-gravimetric method to determine SWC at this precise time. We can see that the direct measurements are matching quite good PlantCare measurements, except from C5.4, which seems to have drifted away in the last part of the measurements.

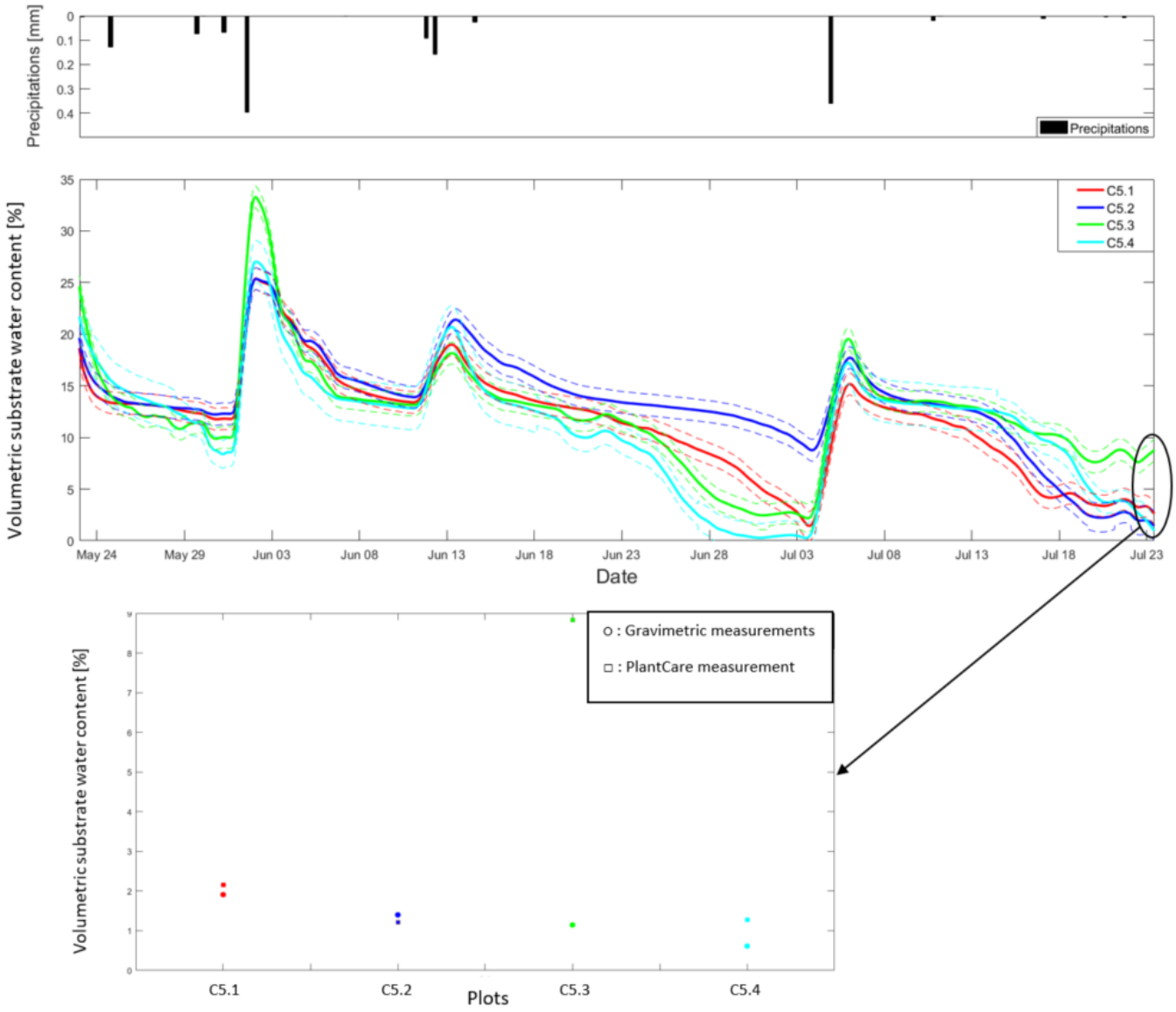

Figure 14: *Evolution of SWC for each quadrats of C5 over time and verification of measurements by gravimetric method at the end of the experiment.*

Based on our conclusions in terms of variability on the plots C5, both in terms of abiotic parameters and on vegetation coverage, we expected a difference in SWC between C5.1 (the highest) and the three others. For example, Buckland-Nicks et al. (2016) showed that the area influenced by spatial structures and thus received shadow, presented the greatest plant cover and the lowest substrate temperature, but also the highest SWC. Our measurements somehow proved to have different behaviours for SWC, while the other parameters (e.g. plant coverage, substrate temperature) are in line with the study. From the 23rd of June to the 3rd of July,

the quadrats C5.3 and C5.4 are dryer than C5.1, as it was expected. However, C5.2 has higher SWC than C5.1, while it was expected that C5.1 should present higher SWC.

Two hypotheses could explain this phenomenon. Firstly, C5.2 has actually higher SWC than C5.1. Indeed, C5.1 is presenting a significant higher coverage than the three others. This higher coverage will results in more water uptake from the roots and thus higher daily moisture loss (Berretta et al., 2014). Thus, even if the abiotic parameters indicates a higher SWC for C5.1, the plants on the quadrats complicate the behaviour of water in the substrate. Indeed, when observing the quadrats one by one we saw that C5.2 has a very limited vegetation coverage, even compared to C5.3 and C5.4. Thus C5.3 and C5.4 present the lower SWC because of effect of radiation and vegetation coverage. Then comes C5.1, with low radiation and high vegetation coverage, resulting in high water uptake. Finally, C5.2 with no much vegetation coverage but high radiation. This hypothesis can be true only if the water uptake by plant is a important parameter, which cannot be verified with actual data. In addition, we think that this hypothesis can only be true in our particular climatic conditions. For instance, for Buckland-Nicks et al. (2016) a lot of rain fell on their plots during their experiment, and thus higher presence of vegetation can positively impact SWC because of the ability of vegetation roots to retain water more (Czemiel Berndtsson, 2010). In our case, with practically no rain event, this function of vegetation roots is not well developed. On the contrary, plants will more have a negative feedback on SWC since they will absorb water for their physiological processes.

The second hypothesis resides in the locality of PlantCare measurements. For instance, if C5.2 was located in an area with more fine matter than the other sensors it would have measured higher SWC. Indeed, at those SWC, the water will not be distributed equally between fine matter and mineral aggregates. Also, if the sensor in C5.1 is near plant roots, the substrate should be dryer in this zone because of water uptake of the plants, while if C5.2 is in an area with no much roots no water uptake is present and the water is lost only by evaporation at this place. This unexpected behaviour can thus be explained bythe locality of PlantCare measurement and/or the presence of plants in the measurement zone.

This gives us an indication that for a such precise monitoring at quadrat scale, our setup can not provide certain measurements, as PlantCare measurements are very local. Indeed, we extrapolate SWC measurements around few centimetres around the probe to a quadrat of one meter square. By example, TDR probes would be more suitable in this application since their volume of influence is greater. Another solutions would be to place more PlantCare in one quadrat, thus avoiding this effect of locality.

4 Conclusion

To put this thesis in a nutshell, the first conclusion is that PlantCare sensors appear to be more suitable than EC-5 for green roofs and their specific substrates composition. As a reminder, EC-5 showed two measurements bias: the steepness of the calibration curve created data overlaps in low SWC and the coefficient of variation was greater than PlantCare for high SWC. The second conclusion is that the difference in substrate depths between both plots induced variations of drying rates and consequently of SWC. As a matter of fact, this difference in SWC also impacted vegetation coverage: 20% of the surface of the deepest plot was covered by plant while only 5% for the shallowest. The last conclusion concerns the spatial heterogeneity of solar radiation explained by the presence of ventilation structures on the roof. On the one hand, this heterogeneity influenced the vegetation coverage: the quadrat that experienced the lowest exposition showed the highest plant coverage. On the other hand, it is more complex to state on the effects of this heterogeneity on SWC given the presence of plants and the sensors' small volume of influence.

4.1 Perspectives

This thesis offers three major areas for future research. The first one concerns the short measurement period and the extraordinary weather conditions of the experiment. Therefore, a longer measurement period could be conducted in order to validate the conclusions of this thesis for different climatic conditions. The second one is the number of sensors installed. Indeed, given the sensors' small volume of influence, it could be more efficient to use 3 to 4 sensors per quadrat. The third and last one is related to the vegetation and the potential of monitoring its evolution over time and in parallel with SWC.

Part II

State of the art & additional information

1 State of the art

1.1 Green roofs

A green roof is defined as a vegetated area that is structurally integrated on top of man made structure, such as houses, towers, facilities. Green roofs have been developed by humans since the fifth century. Their aesthetic value was appraised by the Babylonian that constructed hanging roof gardens and by the ancient Mesopotamian civilization who built them in their ziggurats (Berardi et al., 2014) . The Romans also implemented roof gardens, for example with the Mysteries villa. Northern European countries were also known for developing houses with vegetation cover, in this case not for their aesthetic value but for thermal insulation. Green roofs were then put aside during the Middle Ages and the regression of knowledge in architecture and art that characterized this era. Green roof technologies were reintroduced in the modern architecture by Le Corbusier and by American organic architects who proposed these infrastructures as a tool to reintegrate nature in cities. Since then, green infrastructures are gaining more and more interest worldwide for their aesthetic value and their natural aspect, but also for their environmental and anthropological benefits. For example, the coverage occupied by green roofs in Germany is increasing by approximately 13.5 millions m^2 each year (Oberndorfer et al., 2007) and 10 % of its buildings are recovered by green areas. Modern green roofs are constructed following this order, from bottom to top: structural deck, separation and thermal insulation layer, waterproof and root barrier, moisture retention material and protection layer, drainage layer, filter layer, growing medium and finally the plants (Vijayaraghavan, 2016). This succesion protects the building from any damages and avoid the stagnation of water which could harm the plants by the development of fungi.

Green roofs can be classified in two types. We first have extensive green roofs that are lightweight, have shallow substrate (50-200 mm of depth) and designed for low need of maintenance. This type is often planted with drought-tolerant perennials and there is usually no need of irrigation because of less water needs. The plants that will grow on those green roofs will be limited in their development compared to natural ecosystems. The coverage and height on those green roofs is low. The second type is known as intensive green roof and is basically a roof garden, with much deeper substrate depth (200-2000 mm) and thus a much higher potential plant diversity. Their use is much wider than extensive green roofs, because they can be recreational, aesthetic, used for growing food or as green open spaces. Extensive type weights less, can be implemented on sloped roofs and is easier to design and to construct, thus they are appropriate for large-sized rooftops. However, the types of plants that can be used is restricted and both the thermal and hydrological performance potentials are lower compared to the intensive type. Typical intensive and extensive green roofs are illustrated in Figure 15.

(a) Extensive

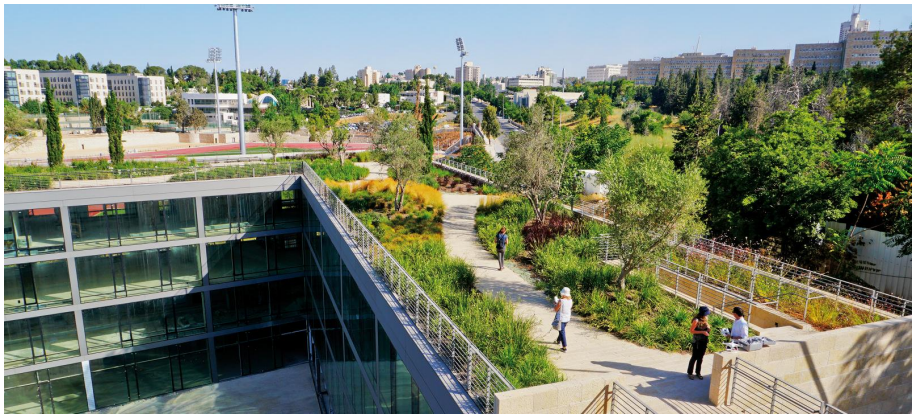

(b) Intensive

Figure 15: *Typical extensive and intensive green roofs (Source: Zinco Ltd.).*

Green roofs create a whole world of scientific research. The research concentrates on the benefits that green roofs can provide. Indeed, these structures are able to respond to a lot of issues. The hydrological performance of green roofs is a subject that received a lot of attention. Researchers study the response of green roofs to rainfall events in terms of runoff and stormwater management. All studies show that green roofs are able to retain rain and thus decrease the total volume of runoff, from the roof scale (Carpenter et al., 2016; Vijayaraghavan et al., 2012) to basin and regional scale (Carter and Jackson, 2007; Versini et al., 2015). Green roofs were also studied in the improvement of runoff water quality (Zhang et al., 2015; Berndtsson et al., 2009). In addition, studies concentrate on the thermal performance of green roofs, which means their ability to reduce the Urban Heat Island effect (which consists in the mean temperature of city centres being significantly warmer than the countryside) (Santamouris, 2014; Susca et al., 2011; Razzaghmanesh et al., 2016). Green roofs were also studied in various benefits, such as air pollution abatement (Yang et al., 2008; Rowe, 2011), noise reduction (Yang et al., 2012; Van Renterghem and Botteldooren, 2009), reduction of energy consumption by isolation (Castleton et al., 2010; Jaffal et al., 2012). The ability of green roofs to reintroduce biodiversity in terms of plants and animals is a highly studied subject, considering green roofs as ecosystems for wild plants (Madre et al., 2014), bees (Colla et al., 2009), birds (Fernandez-Canero and Gonzalez-Redondo, 2010), varied insects (Schindler et al., 2011) or event bats (Pearce and Walters, 2012).

We can notice the important amount of papers that can be found on green roofs. Studies that are similar to this thesis are nevertheless quite rare or only concerne a part of the scope. Kargas et al. (2013) focused their work on the quantification of the accuracy of dielectric moisture sensors in green roofs substrate. Their work was thus very useful in the preparation of our calibration protocol. Concerning the effect of substrate depth on soil moisture content and on vegetation development, a good diversity of scientific papers can be found. Nardini et al. (2012) compare the development of shrubs versus herbaceaous for two substrate depths, and show that both the substrate depth and type of vegetation have an impact on runoff reduction capacity. Dunnett et al. (2008) conducted a long term study (6-year study) on two substrate depths (100 and 200 mm) about the dynamics of planted and colonising species. Their results show a greater survival, diversity, size and flowering for deeper depths, while the bare ground and mosses cover were found on shallower plots. They also demonstrate that the different results obtained between first years and final years of the experiment proved a need for long-term monitoring of green roof behaviour. Buckland-Nicks et al. (2016) studied a very similar case, by trying to quantify the effects of spatial heterogeneity in solar radiation and substrate depth. In their case, an atrium was introducing a shadow heterogeneity on a roof. They show that the difference in radiation introduce changes in substrate temperature and substrate water content, having a consequence on the vascular plants cover. However, multiple factors were different than in the scope of this thesis such as the climate (cold, humid, maritime), the mix of plants, type of substrate, etc.

1.2 Green roofs & biodiversity

Green roofs are considered as quite low biodiversity ecosystems (Brenneisen, 2006), since most of extensive green roofs are limited in sedum species. However, to maximize ecological functions of green roofs, varied and heterogeneous designs should be implemented within a city (Francis and Lorimer, 2011). In addition, diverse species composition should be implemented to provide maximum ecological function of green roofs. This diversity in green roofs has additional advantages, it does not only maximize ecological functions. For instance, diverse ecosystems on green roofs are theoretically more resistant and resilient to stresses (Cook-Patton and Bauerle, 2012). This means that diverse extensive green roofs under dry conditions will have a higher survival rate and a better aesthetic value (Nagase and Dunnett, 2010). To promote biodiversity on green roofs, multiple actions can be undertaken. Creating spatial heterogeneity is one of them. For this purpose, varying substrate depth can create spatial heterogeneity (Brenneisen, 2006) as substrate depth is the principal factor for plant diversity(Madre et al., 2014). Another way to promote spatial heterogeneity is to implement shadow areas on the roof. This will create plants mixes as the conditions on the shadowed areas and illuminated areas are not the

same (Buckland-Nicks et al., 2016). Finally, using native plants is recommended since they are adapted to the local climatic conditions (Monterusso et al., 2005) and that indigenous species present more interactions with local fauna.

In this focus to promote local biodiversity into urban areas, the possibility of green roofs to act as habitat analogues was studied. This kind of habitat is inspired from a reference natural ecosystem that is similar in terms of composition, structure and mechanisms (Lundholm and Richardson, 2010). Thus the flora present on the roof could be inspired by natural ecosystems with similar abiotic conditions. Indeed, green roofs presents similarities in their conditions to certain natural ecosystems. The principal conditions that define extensive green roofs are: dry conditions due to shallow substrate (Farrell et al., 2012), high fluctuations in substrate temperature, water scarcity and high exposure to wind and sun (Nagase and Dunnett, 2010). Some ecosystems in the wild present such conditions: it is the case of rockery dry grasslands (Lundholm and Richardson, 2010; Lundholm, 2006). In belgium, we can find dry calcareous grasslands that present similar conditions.

1.3 Soil Water Content

Water in soils is one of the most important parameters that controls physical, chemical and biological processes that occur in natural soils and artificial substrate (de Rooij, 2004). Water can physically act both as a lubricant and as a binding agent, therefore water content in the soil is a parameter that has an influence on the strength of soil and its structural stability. From a chemical point of view, water acts as a transport agent for dissolved minerals and suspended biological components, thus playing a considerable role in soil formation and deterioration. Finally, all living organisms depend of water, all biological production from soil, either as crops, forests or grasslands, indeed depends highly on water availability in their growing medium.

Water of the soil is found under three different forms: gravitational, capillary and hygroscopic water (Susha Lekshmi et al., 2014). Gravitational moisture is the free water that will percolate through the soil in response to gravitational forces. This water stands in the macro-pores of the soil and its flow through the profile is quite quick, typically 2-3 days after a rainfall or an irrigation. This water is then usually not considered as plant-available moisture since its presence in the soil quickly disappear. On the contrary, the capillarity water is held within the micro-pores of the soil due to the force of adhesion and cohesion, which counter gravity. This water is available and responsible for physical, chemical, mineralogical and biological processes in the plant-soil-atmosphere continuum. Indeed, the micro-pores allow water to stay in the soil while letting it available for plant absorption. Finally, the hygroscopic moisture is a thin water film formed around the surface of soil particles. This water is not available for plants since it is held by very strong adhesion forces, as a consequence to its position on the surface of particles.

In order to seize better soil water content-plants interactions, Widtsoe and McLaugghlin (1912) were the first to present capillarity water as field water capacity or optimum capillary water capacity which represents the water that is available for the plants. Field water capacity is the water still present into the soil after gravitational water was drained away: this is the highest amount of water to allow best plant growth. On another hand, the wilting point, or the hygroscopic water coefficient, is the amount of water below which plants will die due to water scarcity. To obtain water contained into the soil that can be absorbed by plants' roots, the subtraction of the field water capacity by the wilting point is operated. All these definitions help rely soil moisture content to plants physiological states.

There are two ways to define water content (Romano, 2014). The first one, the more traditional and ancient one, is the ratio of the mass of water contained by the sample before oven-drying to the sample mass after it has been dried, until reaching a constant mass. The second definition uses the volume of water contained in a volume of soil. Both definitions give a dimensionless ration or a percentage, but since these two definitions do not provide the same exact information, it is important to specify which definition is used. However, it is quite simple to exchange ratio of masses to ratio of volumes and the opposite, provided that the bulk density of the soil ($\rho_b, [kgm^{-3}]$) and the density of water ($\rho_w, [kgm^{-3}]$) are know, by the formula

$$\theta_v = (\rho_b/\rho_b)\theta_m$$

with θ_v the volumetric water content $[m^3m^{-3}]$ and θ_m the gravimetric water content $[kgkg^{-1}]$.

When all the pores are filled with water, a state called full saturation is reached. The water content at saturation, θ_s, is always lower or equal to soil porosity (η). This is the maximum water content that a soil can reach.

The presence of stones or mineral fragments in a soil or substrate will influence its properties, and particularly its water retention and hydraulic conductivity. The presence of rock fragments in the soil reduces the total volume of soil that is available for water flow. This results in higher maxima and lower minima after a rain event, but also in a reduction of the total soil water storage (Hlaváčiková et al., 2018). Mineral aggregates can also complicate the measurement of soil moisture. On the one hand, the presence of large stones is problematic for sensor installation and, on the other hand, the interpretation of measured values is also an issue.

1.4 Soil moisture measurement methods

Methods for soil water content measurement are multiple and diverse. We propose here a quick review of the most often used techniques, with a particular focus on the one that are used on green roofs.

1.4.1 Direct measurements

Direct measurements consist of first a removal or separation of the water from the soil matrix and then of measuring directly the amount of removed water.

The thermo-gravimetric method is the most direct, precise and widely used technique. This technique is often seen as a reference procedure. It consists of sampling soil on the field and then determining the water content by comparison of wet and dry mass of the sample. The wet weight is obtained by simple weighing just after sampling, the dry mass is obtained after oven-drying the sample for 24 hours at 105 °C or for 48 hours at 60 °C. To achieve perfect drying, it is advised to continue drying until no more changes in mass are detected. If the soil sample contains a large amount of organic matter, it is advised to choose the lowest temperature since higher temperature could volatilize organic matter (Susha Lekshmi et al., 2014).

The main advantage of this method is its accuracy and the fact that it is always working. However, there are a lot of disadvantages: it is a destructive method ; the access to a laboratory and samplings tools might constitute a constraint ; this method is time consuming since you have to oven-dry the samples ; it is impossible to engage continuous measurement and to measure at the exact same location etc. Nevertheless, it constitutes a really effective method as it allows measurements verification.

1.4.2 Indirect measurements

Those techniques consist in measuring physical or physico-chemical properties of the soil or substrate, properties that need to be highly correlated with water content. Those methods are in general non-destructive and thus allow continuous measurements on the same location. The main disadvantage of indirect measurements lies in that they often need specific calibration curves in order to link their measurement to soil water content and show a representative soil moisture. We will now outline the principle indirect methods used to measure soil water content, with a specific scope on the methods that were used on green roofs.

The Time Domain Reflectometry (TDR) technology uses metallic probes (2-3 rod) that send Electromagnetic (EM) pulses in the soil along the waveguides. The propagation velocity (v) of these pulses is then determined by measuring the travel time to cover the distance of the

wageguides, and is related to apparent dielectric properties of the substrate surrounding the probe, thus on soil moisture content (Dobriyal et al., 2012). Indeed, water has a high dielectric permittivity ($\varepsilon_w = 80$) in comparison with mineral soil solids ($\varepsilon_s = 2 - 9$) and air ($\varepsilon_a = 1$). This method, which is the most widely used technique for soil moisture measurement (Kelleners et al., 2004), is the subject of many papers, from soil moisture measurement on forest soil (Gray and Spies, 1995) to corn field (Topp and Davis, 1985) or deserts (Alvarez-Benedi et al., 2005). In addition, a lot of papers used TDR for measurement of SWC on green roofs, such as Fioretti et al. (2010) that installed TDR probes for monitoring of SWC. Getter et al. (2011) also showed that TDR probes produce semi-qualitative measurements because of the presence of air pockets in the substrate. Indeed, green roofs are constructed using artificial substrate, substrate that is often rich in mineral aggregates such as stones, crushed bricks or mineral aggregates. This composition can alter measurements with dielectric sensor, as the presence of stones can change the architecture of the sensors by a deviation of the waveguides thus altering the transmission of EM pulses (Souto et al., 2008)

Frequency Domain Reflectometry (FDR) method uses an oscillating current. The sensor can also be considered as a capacitor, the 2 or 3 probes acting as two opposing metal plates and the soil or substrate acting as a dielectric medium between them (Linmao et al., 2012). The oscillating current will flow through the system, but the current will be attenuated by the capacitance of the soil. The capacitance of the soil/substrate can be computed from the voltage and current of the system (V=C*I). After this, the capacitance is related to the dielectric constant of the soil and thus its moisture. In fact, the working principle of FDR is similar to capacitive sensor that will be detailed hereunder, except that FDR uses a wide range of frequency (Susha Lekshmi et al., 2014). The only available study that used FDR for SWC measurements is from Kargas et al. (2013). Their results showed that the permittivity and soil moisture on green roofs were linearly linked, with high R^2 for all tested substrates (Kargas et al., 2013). It was however necessary to achieve a calibration for every substrate. This method thus shows promising results for future application on green roofs.

1.5 EC-5

The first soil moisture sensor that was used for the experiment is the ECH_2O EC-5 from Decagon Devices. The sensors uses the capacitance based method, this method nowadays attracting more interest because of the development of high-quality and low-cost high-frequency oscillators (Kelleners et al., 2004). The method is based on the strong dependence of EM signal on volumetric water content of soil. Indeed, as mentioned in the TDR technology, water has a relatively large dielectric value compared to the one of air and soil. The basic principle of this method is to include a dielectric medium, which is the soil or the substrate, as a

element of the dielectric of the sensor capacitor. The whole capacitance of the sensor consists then in the capacitance of the medium (C) and the capacitance C_s due to stray electric fields (Kelleners et al., 2004). The sensor measure the dielectric permittivity of the substrate or soil surrounding the probe, with a volume of influence of around 300 cm^3. The sensors also includes an electronic oscillator that produces waves with a specific high frequency (70 MHz for EC-5). Soil dielectric permittivity is determined by measuring the charging time of a capacitor using the soil or substrate as a dielectric medium, from a starting voltage (V_i) to a final voltage (V_f) by applying a voltage (V) (Bogena et al., 2007). The parameters R (resistance), V_i and V are maintained constant during all measurements, thus the charging time of the capacitor, t, is related to the capacitance by:

$$t = RC\ ln\ \frac{(V_f - V + V_i)}{(V_i - V)} \tag{3}$$

The capacitance is a function of both the dielectric permittivity (ε) of the substrate or soil and by a geometrical factor, g, which indicates the electrode configuration and the EM field shape. The capacitance can then be computed as:

$$C = g\varepsilon \tag{4}$$

Finally, the dielectric permittivity can be computed as follows, if we assume that the charging time of the capacitor is a linear function of the dielectric permittivity of the substrate/soil:

$$\frac{1}{\varepsilon} = \frac{1}{t}\ [Rg\ ln(\frac{V_f - V + V_i}{V_i - V})] \tag{5}$$

The dielectric permittivity, which is related to SWC , has an impact on the shape of the charging curve. When SWC is high, the charging time of the capacitor will be longer, which results in a flatter charge curve than at inferior contents. In conclusion, the capacitor which uses as a medium a soil/substrate with high SWC will reach the threshold voltage of the capacitor in a longer time than for dry medium, as shown is Figure 16. By linking this output to the average voltage over the pulse length (Δt), we will get a high output of the sensor if the SWC is high, and the contrary when the soil is drier. After this, we will have to create calibration curve to link the voltage outputs to volumetric water content, as it was realized in this experiment.

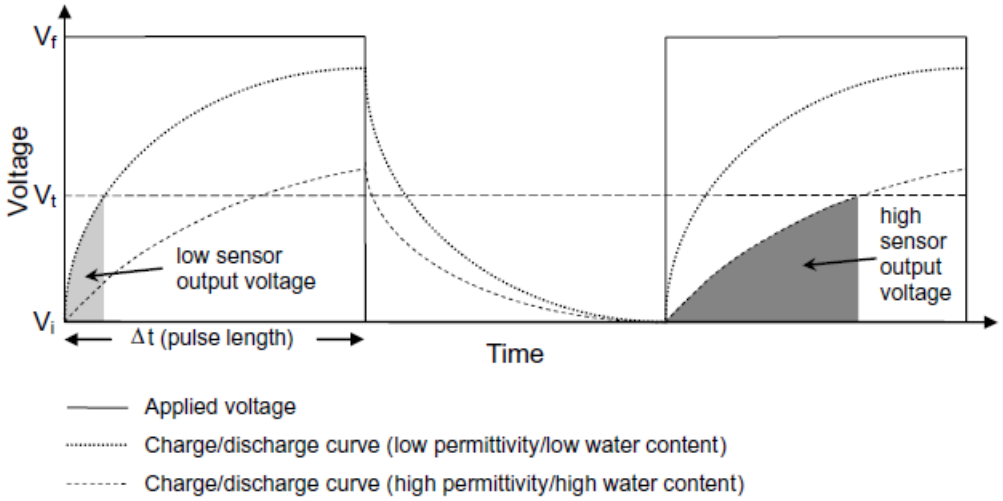

Figure 16: *Charge and discharge curves of two capacitors: one with high SWC medium and the other with low SWC (Bogena et al., 2007).*

Few studies used this capacitive sensors to monitor substrate water content on green roofs experiment, but none of them tried to understand the accuracy that these sensors have on ths substrates of green roofs. Nardini et al. (2012) used the sensors to rely the difference in SWC with substrate depth and the maximum δT. **?** utilize EC-5 but used a standard calibration function, the one of perlite. We can see that these use were the not the center of those papers and thus no specific work was done to test the ability of these sensors on greens roofs.

1.6 Plant-Care

The second soil moisture sensor that was used is the 'PlantCare OEM Soil Moisture Sensor' from PlantCare Ltd (Russikon, Switzerland). It comprises a heat pulse generator and a temperature sensor (Matile et al., 2013) integrated in an especially developed felt material. This felt is in moisture balance with the soil and acts as the interface between surrounding substrate and the sensors. The measurement method is divided into two phases: first, the sensor is heated up by 2-3 °C for 20 seconds, the temperature rise depending on the water content of the felt but also the ambient temperature, since heat conductivity is highly dependent of temperature. Reece (1996) found that this temperature rise was mainly a function of the water content and used it for the calibration of matrix potential for a heat dissipation sensor technology. On the contrary, PlantCare sensor is measuring the time after which the maximum temperature has fallen to a threshold temperature, which is more or less 20 % of the temperature rise. The cooling time is dependant on the thermal conductivity of the substrate around the sensor. Merely, if the soil moisture level is high, the cooling-down period is short. In contrast, if the substrate is dry, the cooling-down period will be much longer. The sensor's cooling-down time thus will provide a reliable evaluation of the SWC. In addition, the high dependence of con-

ventional heat dissipation sensors (Flint et al., 2002) is avoided by this new procedure, which was tested with the temperature correction that was achieved for this sensors in the experiment.

Figure 17: *A: PlantCare sensors ; B: sensor without the synthetic felt (Matile et al., 2013).*

We were not able to find any papers that used PlantCare sensors in a green roof experiment. This reinforce the pertinence of testing PlantCare in our experiment.

2 Additional informations

This section aims to thoroughly describe elements that were not essential to the global comprehension of this thesis but still needed to be clarified.

2.1 Temperature sensitivity of PlantCare

Through this experience, we tested the PlantCare sensitivity to temperature changes. For this purpose, we led another laboratory experiment. We proceeded the same way as before to determine the exact SWC. However in this case the goal was not to study the reaction of sensors to the addition of water, but to determine for a given SWC, how the measurements change in function of the substrate temperature. Therefore, we heated the substrate up to 60 °C, quickly prepared the column with this hot substrate and placed the sensors into the column. We carried out this experiment for the most frequently encountered SWC in our caset, which means from 0% to 20 %. The temperature range was included the maximum temperature that was observed during the measurements (40 °C) and the minimum (20 °C). Figure 18 expresses the result of this experiment.

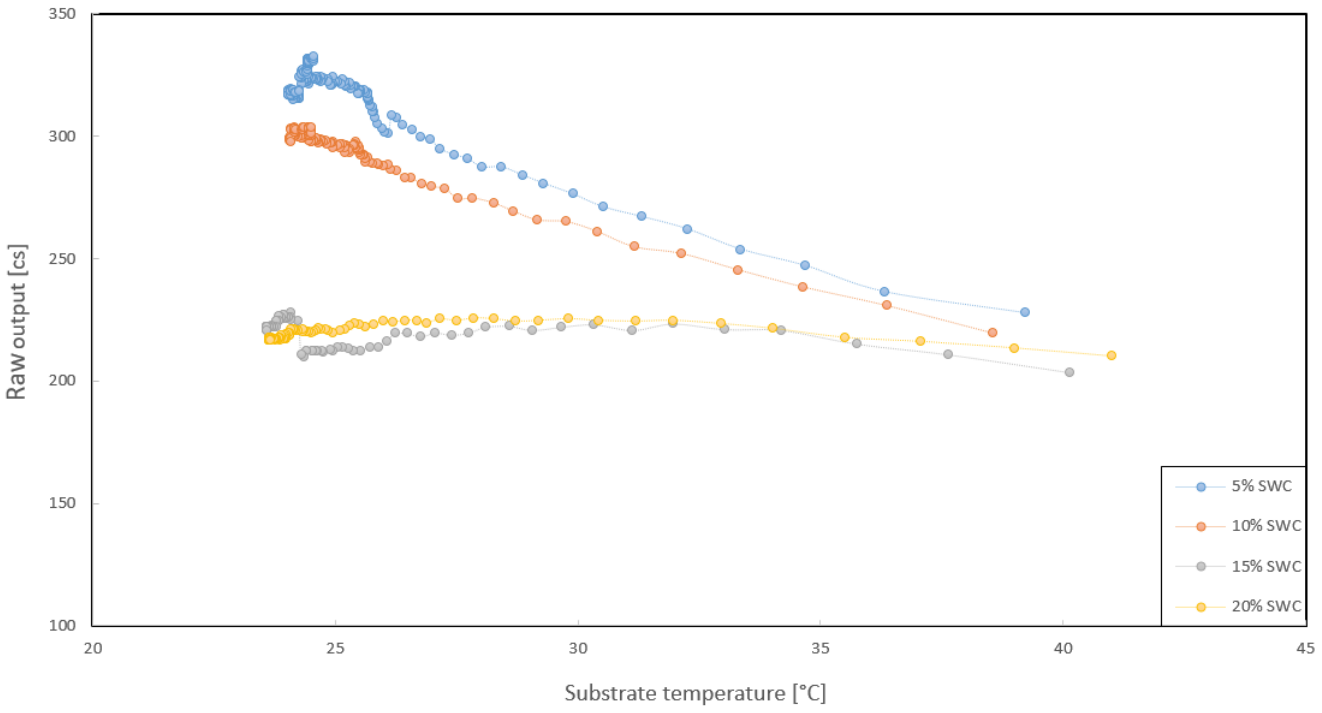

Figure 18: *Evolution of PlantCare outputs in function of the temperature for 4 steps of SWC.*

We can encounter two different behaviours here. For 15 and 20 %, we can notice equal measurements for high and low temperature, thus no temperature sensitivity is present at those SWC. For 5 and 10% SWC, we can see that the measurements are different for high and low temperatures. Thus, we can notice that the PlantCaren sensor is sensitive to temperature when low SWC are encountered. However, we believe that this behaviour to be exacerbated by the time of equilibrium at those SWC. Indeed, the first measurement (at 40 °C) occurs just

after (30 min) the sensors were put in the column. When considering those SWC, the sensors take some time to equilibrate with the substrate, since the felt was dipped into water before insertion. Thus, we verified this temperature sensitivity at low SWC with field measurements on the field. We selected a typical period of measurement where the SWC was lower than 10 % and showed the evolution of measurements with the evolution of substrate temperature (Figure 20).

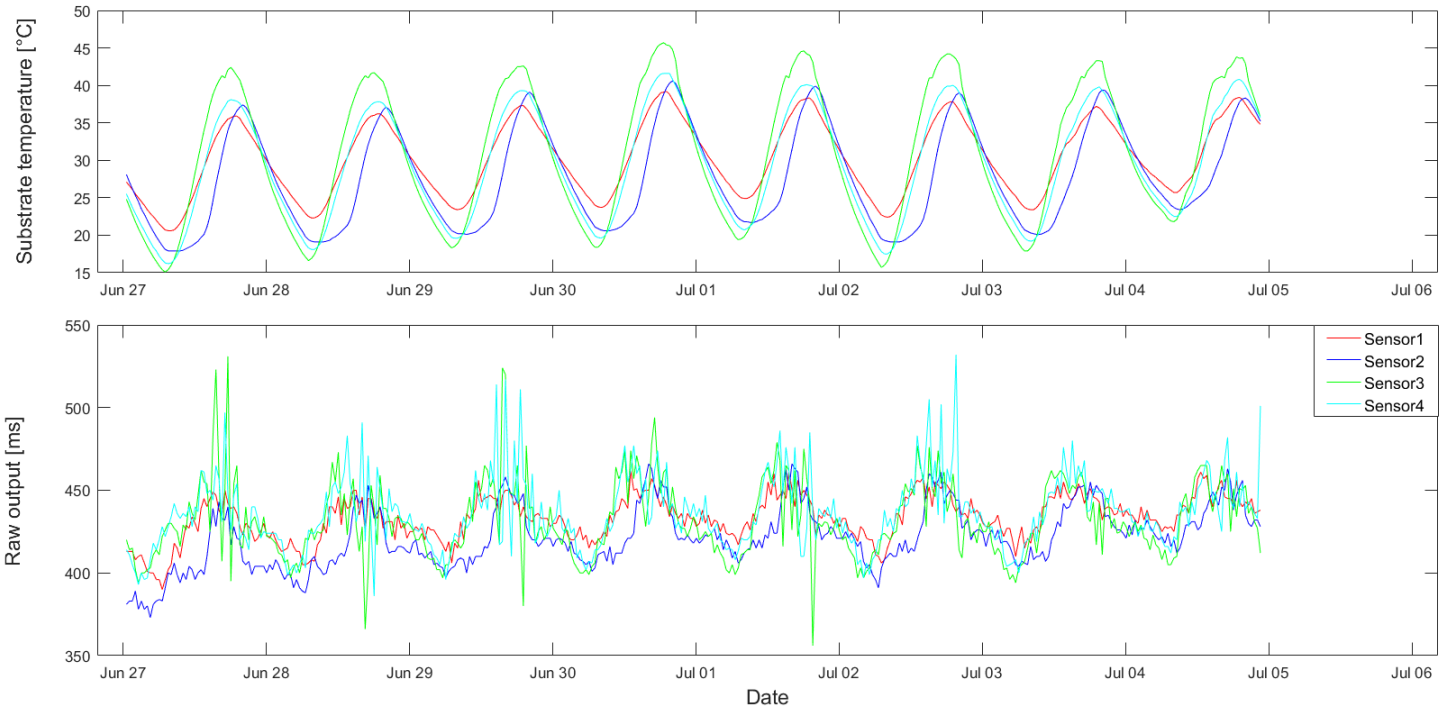

Figure 19: *Evolution of Plantcare outputs for a period of 9 days in function of the evolution of temperature.*

This graph indicates that indeed, the PlantCare is sensitive to temperature at the discussed SWC, since the measurements oscillate with the evolution of temperature through the day, with an amplitude of around 50 cs, which corresponds to a difference of 5% SWC. We also carried out this operation for higher SWC and this confirmed that after 10 %, the PlantCare is highly less sensitive to temperature change in the substrate. This confirmed that a correction of temperature sensitivity is needed for the PlantCare in such shallow substrate depth, as it was mentioned by Matile et al. (2013). On another side, Assouline et al. (2010) showed that the diurnal dynamics could have a physical explanation, which would be induced by the evaporation at the surface and the redistribution of water in-depth due to temperature gradient dynamics. This subject should then receive more attention. However, we corrected this temperature sensitivity by smoothing the curve ant thus avoiding this temperature effect by taking the means values.

2.2 Plant coverage measurements

This section presents the two different methodologies that were developed in order to measure the plants' responses, in terms of vegetation coverage, to conditions present on the plots.

2.2.1 Neural Network algorithm

The pictures were taken by a drone DJI Phantom 4 that was equipped with a RGB camera. Different heights were tested in order to have the best quality that was possible with this drone. The pictures were taken the 29th of June.

This segmentation is based on Artificial Neural Network (ANN), which are computing systems that were inspired by biological neural networks. Those systems learn to perform tasks by considering examples. For instance, in image segmentation, we give the algorithms examples of plants and substrate under the form of groups of pixels. Based on this, the network will train on these examples in order to be able to distinguish plants and substrate in a new image. In our case, the network will be very efficient because its training and test are the same image, thus the conditions for segmentation are optimal. In order to provide the necessary information for a future use of the network, the MATLAB script is provided in the Appendice 3.

The segmentation is working following this procedure, following the order of the script: first, the image is imported in the working space. After this, the execution of the code will open the imported image in order to train the network: polygons containing pixels of plants, substrate and shadow need to be sampled by the operator. The network will then construct different vectors containing the information. Then, the script constructs target and train, which are two matrices that will train the network to separate the different parts of the image. From this, the toolbox 'nprtool' from MATLAB is launched, it will use the train and target to create a neural network as a MATLAB script. This leads to the last part of the script, where we use the neural network to classify the plants and the substrate on the image. The value 1 in this segmentation is related to the plants pixels and the 0 everything that is not recognized as a plant. Finally, the last part of the script allows us to deconstruct the small round aggregates that were mistakenly segmented. Based on these informations and the script present in the appendixes, this must allow future user an easier utilization.

2.2.2 Point-quadrat measurements

This work has been achieved by Julie Reniers in her Master's thesis. It is important to make a brief description of her methodology in order to understand correctly the conclusions of this thesis.

The measurements occurred from the 26th to 29th of June (a few days before thedrone pictures). This method was used because of its recognized efficiency for grassland application. This method consists in identifying the species present in 100 equidistant points of the quadrat

($1m^2$). To do so, a device is elevated and perforated with 100 holes. A needle is then lowered in every hole, if the needle touch a plant, the specie is identified.

Figure 20: *Point-quadrat device for measurement of relative plant coverage (Credits: Julie Reniers).*

From there, the relative coverage is obtain by

$$Relative\ coverage = \frac{Number\ of\ needles\ touching\ the\ specie}{Total\ number\ of\ needles} * 100 \tag{6}$$

To study the effect of the radiation (qualitative, fix, 3 modalities) and the substrate depth (qualitative, fix, 2 modalities) on vegetation coverage, a crossed variance analysis with two factors was conducted. A first operation was applied to consider the random effects due to the quadrat and its position in the data set. After that, when no interaction between factors was observed, an analysis of the variance with a single factor (radiation or substrate depth) was conducted with RStudio software. This analysis was also conducted specifically in the quadrat containing our sensors in order to compare both datas.

Application conditions were also tested before this analysis. However, some species and their transformed variable did not respect the condition of variance equality. Thus, the variables were not transformed because the transformations presented lower p-value (Levene test) than untransformed variables. One specie did not respect this test of variance equality *K. Macrantha*. The results of variance analysis were still included but need to be considered with precaution due to their possible tendencies for this specie.

References

Allen, R. G., Pereira, L. S., Raes, D., Smith, M., and Ab, W. (1998). Crop Evapotranspiration - Guidelines for computing crop water requirements - FAO Irrigation and drainage paper 56. pages 1–15.

Alvarez-Benedi, J., Munoz Carpena, R., and CRC Press. (2005). *Soil-water-solute process characterization : an integrated approach*. CRC Press.

Assouline, S., Narkis, K., Tyler, S., Lunati, I., Parlange, M., and Selker, J. S. (2010). On the Diurnal Soil Water Content Dynamics during Evaporation using Dielectric Methods. *Vadose Zone Journal*, 9(3):709.

Beaudet, M. and Messier, C. (1998). Growth and morphological responses of yellow birch, sugar maple, and beech seedlings growing under a natural light gradient. *Canadian Journal of Forest Research*, 28(7):1007–1015.

Berardi, U., GhaffarianHoseini, A. H., and GhaffarianHoseini, A. (2014). State-of-the-art analysis of the environmental benefits of green roofs. *Applied Energy*, 115:411–428.

Berndtsson, J. C., Bengtsson, L., and Jinno, K. (2009). Runoff water quality from intensive and extensive vegetated roofs. *Ecological Engineering*, 35(3):369–380.

Berretta, C., Poe¨, S., and Stovin, V. (2014). Reprint of "Moisture content behaviour in extensive green roofs during dry periods: The influence of vegetation and substrate characteristics". *Journal of Hydrology*, 516:37–49.

Berry, B. J. L. and Okulicz-Kozaryn, A. (2011). An Urban-Rural Happiness Gradient. *Urban Geography*, 32(6):871–883.

Bogena, H. R., Huisman, J. A., Oberdörster, C., and Vereecken, H. (2007). Evaluation of a low-cost soil water content sensor for wireless network applications. *Journal of Hydrology*, 344(1-2):32–42.

Brenneisen, S. (2006). Space for urban wildlife: Designing green roofs as habitats in Switzerland. *Urban Habitats*, 4(1):27–36.

Buckland-Nicks, M., Heim, A., and Lundholm, J. (2016). Spatial environmental heterogeneity affects plant growth and thermal performance on a green roof. *Science of the Total Environment*, 553:20–31.

Carpenter, C. M., Todorov, D., Driscoll, C. T., and Montesdeoca, M. (2016). Water quantity and quality response of a green roof to storm events: Experimental and monitoring observations. *Environmental Pollution*, 218:664–672.

Carter, T. and Jackson, C. R. (2007). Vegetated roofs for stormwater management at multiple spatial scales. *Landscape and Urban Planning*, 80(1-2):84–94.

Castiglia Feitosa, R. and Wilkinson, S. (2016). Modelling green roof stormwater response for different soil depths. *Landscape and Urban Planning*, 153:170–179.

Castleton, H. F., Stovin, V., Beck, S. B. M., and Davison, J. B. (2010). Green roofs; Building energy savings and the potential for retrofit. *Energy and Buildings*, 42(10):1582–1591.

Chenot, J., Gaget, E., Moinardeau, C., Jaunatre, R., Buisson, E., and Dutoit, T. (2017). Substrate composition and depth affect soil moisture behavior and plant-soil relationship on Mediterranean extensive green roofs. *Water (Switzerland)*, 9(11):1–16.

Cobos, D. R. and Chambers, C. (2005). Application Note Calibrating ECH 2 O Soil Moisture Sensors. pages 1–5.

Colla, S. R., Willis, E., and Packer, L. (2009). Can green roofs provide habitat for urban bees (Hymenoptera : Apidae) ? *Cities and the Environment*, 2(1):1–20.

Cook-Patton, S. C. and Bauerle, T. L. (2012). Potential benefits of plant diversity on vegetated roofs: A literature review. *Journal of Environmental Management*, 106:85–92.

Czemiel Berndtsson, J. (2010). Green roof performance towards management of runoff water quantity and quality: A review. *Ecological Engineering*, 36(4):351–360.

de Rooij, G. H. (2004). Methods of soil analysis: Part 4. physical methods. *Vadose Zone Journal*, 3(2):722–723.

Dobriyal, P., Qureshi, A., Badola, R., and Hussain, S. A. (2012). A review of the methods available for estimating soil moisture and its implications for water resource management. *Journal of Hydrology*, 458-459:110–117.

Dodman, D. (2009). Blaming cities for climate change? An analysis of urban greenhouse gas emissions inventories. *Environment and Urbanization*, 21(1):185–201.

Dunnett, N., Nagase, A., and Hallam, A. (2008). The dynamics of planted and colonising species on a green roof over six growing seasons 2001-2006: Influence of substrate depth. *Urban Ecosystems*, 11(4):373–384.

Farrell, C., Mitchell, R. E., Szota, C., Rayner, J. P., and Williams, N. S. (2012). Green roofs for hot and dry climates: Interacting effects of plant water use, succulence and substrate. *Ecological Engineering*, 49:270–276.

Fernandez-Canero, R. and Gonzalez-Redondo, P. (2010). Green roofs as a habitat for birds: A review.

Fioretti, R., Palla, A., Lanza, L. G., and Principi, P. (2010). Green roof energy and water related performance in the Mediterranean climate. *Building and Environment*, 45(8):1890–1904.

Flint, A. L., Campbell, G. S., Ellett, K. M., and Calissendorff, C. (2002). Calibration and Temperature Correction of Heat Dissipation Matric Potential Sensors. *Soil Science Society of America Journal*, 66(5):1439.

Francis, R. A. and Lorimer, J. (2011). Urban reconciliation ecology: The potential of living roofs and walls. *Journal of Environmental Management*, 92(6):1429–1437.

Getter, K. L., Bradley Rowe, D., and Cregg, B. M. (2009). Solar radiation intensity influences extensive green roof plant communities. *Urban Forestry and Urban Greening*, 8(4):269–281.

Getter, K. L. and Rowe, D. B. (2006). The role of extensive green roofs in sustainable development. *HortScience*, 41(5):1276–1285.

Getter, K. L., Rowe, D. B., Andresen, J. A., and Wichman, I. S. (2011). Seasonal heat flux properties of an extensive green roof in a Midwestern U.S. climate. *Energy and Buildings*, 43(12):3548–3557.

Gray, A. N. and Spies, T. A. (1995). Water content measurement in forest soils and decayed wood using time domain reflectometry. *Canadian Journal of Forest Research*, 25:376–385.

Haferkamp, M. R. (1988). Environmental factors affecting plant productivity.

Hlaváčiková, H., Novák, V., Kostka, Z., Danko, M., and Hlavčo, J. (2018). The influence of stony soil properties on water dynamics modeled by the HYDRUS model. *Journal of Hydrology and Hydromechanics*, 66(2):181–188.

Jaffal, I., Ouldboukhitine, S. E., and Belarbi, R. (2012). A comprehensive study of the impact of green roofs on building energy performance. *Renewable Energy*, 43:157–164.

Jiang, L. and Hardee, K. (2011). How do Recent Population Trends Matter to Climate Change? *Population Research and Policy Review*, 30(2):287–312.

Kargas, G., Ntoulas, N., and Nektarios, P. A. (2013). Moisture content measurements of green roof substrates using two dielectric sensors. *HortTechnology*, 23(2):177–186.

Kelleners, T. J., Soppe, R. W. O., Robinson, D. a., Schaap, M. G., Ayars, J. E., and Skaggs, T. H. (2004). Calibration of Capacitance Probe Sensors using Electric Circuit Theory. *Soil Science Society of America Journal*, 68(2):430.

Linmao, Y., Longqin, X., Guangzhou, Z., Haibo, C., Likuai, S., Zhigang, W., Gouhe, Y., Yanbin, W., Sujun, N., Jin, Y., and Qi, J. (2012). FDR Soil Moisture Sensor for Environmental Testing and Evaluation. *Physics Procedia*, 25(May):1523–1527.

Lundholm, J. T. (2006). Green roofs and facades: a habitat template approach. *Urban Habitats*, 4(1):87–101.

Lundholm, J. T. and Richardson, P. J. (2010). Habitat analogues for reconciliation ecology in urban and industrial environments. *Journal of Applied Ecology*, 47(5):966–975.

Madre, F., Vergnes, A., Machon, N., and Clergeau, P. (2014). Green roofs as habitats for wild plant species in urban landscapes: First insights from a large-scale sampling. *Landscape and Urban Planning*, 122:100–107.

Matile, L., Berger, R., Wächter, D., and Krebs, R. (2013). Characterization of a new heat dissipation matric potential sensor. *Sensors (Switzerland)*, 13(1):1137–1145.

Mentens, J., Raes, D., and Hermy, M. (2006). Green roofs as a tool for solving the rainwater runoff problem in the urbanized 21st century? *Landscape and Urban Planning*, 77(3):217–226.

Monteith, J. L. (1965). Evaporation and environment.

Monterusso, M. A., Bradley Rowe, D., and Rugh, C. L. (2005). Establishment and persistence of Sedum spp. and native taxa for green roof applications. *HortScience*, 40(2):391–396.

Mueller-Dombois, D. and Sims, H. (1966). Response of Three Grasses to Two Soils and a Water Table Depth Gradient. *Ecology*, 47(4):644–648.

Nagase, A. and Dunnett, N. (2010). Drought tolerance in different vegetation types for extensive green roofs: Effects of watering and diversity. *Landscape and Urban Planning*, 97(4):318–327.

Nardini, A., Andri, S., and Crasso, M. (2012). Influence of substrate depth and vegetation type on temperature and water runoff mitigation by extensive green roofs: Shrubs versus herbaceous plants. *Urban Ecosystems*, 15(3):697–708.

Oberndorfer, E., Lundholm, J., Bass, B., Coffman, R. R., Doshi, H., Dunnett, N., Gaffin, S., Köhler, M., Liu, K. K. Y., and Rowe, B. (2007). Green Roofs as Urban Ecosystems: Ecological Structures, Functions, and Services. *BioScience*, 57(10):823–833.

Pearce, H. and Walters, C. L. (2012). Do Green Roofs Provide Habitat for Bats in Urban Areas? *Acta Chiropterologica*, 14(2):469–478.

Raes, D. (2009). The ETo Calculator Table of Contents - Reference Manual. *Fao*, pages 1–38.

Razzaghmanesh, M., Beecham, S., and Salemi, T. (2016). The role of green roofs in mitigating Urban Heat Island effects in the metropolitan area of Adelaide, South Australia. *Urban Forestry and Urban Greening*, 15:89–102.

Reece, C. F. (1996). Evaluation of a Line Heat Dissipation Sensor for Measuring Soil Matric Potential. *Soil Science Society of America Journal*, 60(4):1022.

Regalado, C. M., Ritter, A., and Rodríguez-González, R. M. (2007). Performance of the Commercial WET Capacitance Sensor as Compared with Time Domain Reflectometry in Volcanic Soils. *Vadose Zone Journal*, 6(2):244.

Romano, N. (2014). Soil moisture at local scale: Measurements and simulations. *Journal of Hydrology*, 516:6–20.

Rowe, D. B. (2011). Green roofs as a means of pollution abatement. *Environmental Pollution*, 159(8-9):2100–2110.

Santamouris, M. (2014). Cooling the cities - A review of reflective and green roof mitigation technologies to fight heat island and improve comfort in urban environments. *Solar Energy*, 103:682–703.

Satterthwaite, D. (2000). Will most people live in cities? *Bmj*, 321(7269):1143–1145.

Scalenghe, R. and Ajmone-Marsan, F. (2009). The anthropogenic sealing of soils in urban areas. *Landscape and Urban Planning*, 90(1-2):1–10.

Schindler, B. Y., Griffith, A. B., and Jones, K. N. (2011). Factors Influencing Arthropod Diversity on Green Roofs Factors Influencing Arthropod Diversity on Green Roofs. *Cities and the Environment*, 4(1):5–20.

Souto, F. J., Dafonte, J., and Escariz, M. (2008). Design and air-water calibration of a waveguide connector for TDR measurements of soil electric permittivity in stony soils. *Biosystems Engineering*, 101(4):463–471.

Susca, T., Gaffin, S. R., and Dell'Osso, G. R. (2011). Positive effects of vegetation: Urban heat island and green roofs. *Environmental Pollution*, 159(8-9):2119–2126.

Susha Lekshmi, S. U., Singh, D. N., and Shojaei Baghini, M. (2014). A critical review of soil moisture measurement. *Measurement: Journal of the International Measurement Confederation*, 54:92–105.

Thuring, C. E., Berghage, R. D., and Beattie, D. J. (2010). Green roof plant responses to different substrate types and depths under various drought conditions. *HortTechnology*, 20(2):395–401.

Topp, G. C. and Davis, J. L. (1985). Measurement of Soil Water Content using Time-domain Reflectrometry (TDR): A Field Evaluation1. *Soil Science Society of America Journal*, 49(1):19.

Turner, W. R., Nakamura, T., and Dinetti, M. (2004). Global Urbanization and the Separation of Humans from Nature. *BioScience*, 54(6):585.

U.N. (2014). World urbanization prospects: Highlights. Technical report, United Nations, Department of Economic and Social Affairs.

U.N. (2017). World Population Prospects: The 2017 Revision, Key Findings and Advance Tables. Technical report, United Nations, Department of Economic and Social Affairs.

Van Renterghem, T. and Botteldooren, D. (2009). Reducing the acoustical façade load from road traffic with green roofs. *Building and Environment*, 44(5):1081–1087.

Versini, P. A., Ramier, D., Berthier, E., and de Gouvello, B. (2015). Assessment of the hydrological impacts of green roof: From building scale to basin scale. *Journal of Hydrology*, 524:562–575.

Vijayaraghavan, K. (2016). Green roofs: A critical review on the role of components, benefits, limitations and trends. *Renewable and Sustainable Energy Reviews*, 57:740–752.

Vijayaraghavan, K., Joshi, U. M., and Balasubramanian, R. (2012). A field study to evaluate runoff quality from green roofs. *Water Research*, 46(4):1337–1345.

Widtsoe, J. and McLaugghlin, W. (1912). Bulletin No . 115 - The Movement of Water in Irrigated Soils. (115).

Yang, H. S., Kang, J., and Choi, M. S. (2012). Acoustic effects of green roof systems on a low-profiled structure at street level. *Building and Environment*, 50:44–55.

Yang, J., Yu, Q., and Gong, P. (2008). Quantifying air pollution removal by green roofs in Chicago. *Atmospheric Environment*, 42(31):7266–7273.

Yang, X. and You, X. (2013). Estimating parameters of van genuchten model for soil water retention curve by intelligent algorithms. *Applied Mathematics and Information Sciences*, 7(5):1977–1983.

Yio, M., Stovin, V., Werdin, J., and Vesuviano, G. (2013). Experimental analysis of green roof detention characteristics. *Water Science and Technology*, 68.

Zhang, Q., Miao, L., Wang, X., Liu, D., Zhu, L., Zhou, B., Sun, J., and Liu, J. (2015). The capacity of greening roof to reduce stormwater runoff and pollution. *Landscape and Urban Planning*, 144:142–150.

Zotarelli, L. and Dukes, M. (2010). Step by step calculation of the Penman-Monteith Evapotranspiration (FAO-56 Method). *Institute of Food and ...*, pages 1–10.

Appendices

Appendix 1: Zinco substrate "Rockery Type Plants-Light"

Figure 21: *Picture of Zinco substrate (Credits: Cédric Bernard).*

Product Data Sheet
System Substrate "Rockery Type Plants-Light"

Order No. 612401 / 612501 / 612601

Enriched with light weight aggregates
System Substrate for extensive green roofs in multiple layer build-up.
The load is reduced by ca. 2 kg/m² per installed cm.

Recycling for a better environment

Technical Data

System Substrate "Rockery Type Plants-Light"

Substrate consisting of Zincolit® Plus-Light (sorted high quality crushed brick with selected mineral aggregates), enriched with Zincohum® (substrate compost enriched with fibre materials). Particularly suitable for extensive green roofs with plant species of the ZinCo plant selection "Rockery Type Plants", which can be established by planting plug plants (e.g. ZinCo Root Ball Plants FB 50). Also suitable for extensive green roofs with seed mixtures (e.g. ZinCo Seed Mixture "Meadow Scents", "Grassy Pasture" or "Country Colours"), which can be established by seed sowing by hand or by hydroseeding.
For optimal plant development the use of an appropriate slow release fertilizer (e.g. ZinCo-Plantfit® 4 M) is recommended (as shown in a special data sheet).

Available in Big Bags, as loose material in lorries and in silo trailers.
Please calculate with a compaction factor of 1.2. That means for every square metre and 10 mm of substrate you order 12 l.

Delivery options	Order No.
in Big Bags	612401
loose on lorry	612501
in silo trailer	612601

Features

- high-quality recycled product
- excellent water retention
- high air content – even at max. water capacity
- frost resistant and stable in structure
- suitable for pumping
- basic component Zincolit® is under constant quality control by the University of Hohenheim

Chemical and Physical Properties

Parameter	Reference Value
Volume weight - dry - at max. water capacity	 800 g/l (+/- 75 g/l) 1200 g/l (+/- 75 g/l)
Maximum water capacity	ca. 40 Vol. %
Water permeability mod. K_f	0.6–70 mm/min
pH value (in $CaCl_2$)	6.5–8.0
Salinity (water extract)	< 2.5 g/l
Organic content	< 65 g/l
Compaction factor	ca. 1.20

Subject to technical alterations and printing errors • First edition 07/2003; Revised 10/2012

ZinCo GmbH
Lise-Meitner-Strasse 2 · 72622 Nürtingen · Germany
Phone +49 7022 6003-0 · Fax +49 7022 6003-100
info@zinco-greenroof.com · www.zinco-greenroof.com

Life on Roofs

ZinCo

Figure 22: *Product Data Sheet of the Substrate from Zinco Ltd.*

Appendix 2: Mix of plants present on the plots

Table 3: *Plants selection from meso-xeric grasslands sowed for this experiment*

Species	Acronym	Type of plants	Vegetative type	Sowing density $[g/m^2]$
Anthoxanthum odoratum	Ant_odo	Mesophile	Perennial	830
Briza media	Bri_med	Mesophile	Perennial	830
Bromus erectus	Bro_ere	Mesoxerophile	Perennial	830
Poa pratensis	Poa_pra	Mesophile	Perennial	830
Anthyllis vulneraria	Ant_vul	Xerophile	Perennial	110
Centaurea scabiosa	Cen_sca	Mesoxerophile	Perennial	110
Daucus carota	Dau_car	Mesophile	Perennial	110
Dianthus carthusianorum	Dia_car	Generalist	Perennial	110
Echium vulgare	Ech_vul	Xerophile	Perennial	110
Hieracium pilosella	Hie_pi	Generalist	Perennial	110
Hypochaeris radicata	Hyp_rad	Mesoxerophile	Perennial	110
Koeleria macrantha	Koe_mac	Generalist	Perennial	110
Leucanthemum vulgare	Leu_vul	Mesophile	Perennial	110
Lotus corniculatus	Lot_cor	Generalist	Perennial	110
Medicago lupulina	Med_lup	Generalist	Bisannual	110
Papaver argemone	Pap_arg	Generalist	Annual	110
Primula veris	Pri_ver	Xerophile	Perennial	110
Rhinantus minor	Rhi_min	Mesophile	Annual	110
Rumex acetosella	Rum_ace	Xerophile	Perennial	110
Sanguisorba minor	San_min	Mesoxerophile	Perennial	110
Scabiosa columbaria	Sca_col	Mesoxerophile	Perennial	110
Silene vulgaris	Sil_vul	Xerophile	Perennial	110
Thymus pulegioides	Thy_pul	Xerophile	Perennial	110
Tragopogon pratensis	Tra_pra	Mesophile	Perennial	110
Verbascum lychnitis	Ver_lyc	Xerophile	Perennial	110
Verbascum thapsus	Ver_tha	Xerophile	Perennial	110
Sedum album	Sed_alb	Xerophile	Perennial	110
Sedum acre	Sed_acr	Xerophile	Perennial	110
Sedum rupestre	Sed_rup	Xerophile	Perennial	110
Centaurea cyanus	Cen_cya	Generalist	Perennial	
Chenopodium album	Che_alb	Generalist	Annual	
Trifolium pratense	Tri_pra	Mesoxerophile	Perennial	
Epilobium tetragonum	Epi_tet	Mesophile	Perennial	
Portulaca oleracea	Por_ole	Xerophile	Annual	

Appendix 3: Script for image segmentation by ANN

```
%Image importation
clear
        Img = importdata('DJI_0012.JPG');
        [ligne,colonne] = size(Img(:,:,1));
plant='plot1';
%Selection of the polygons
l = 0;
close all
'Plante'
for i = 1:5
     close()
    maskPlante{i}= roipoly(Img);
end
'Sol'
for i = 1:3
    close()
   maskSol{i}= roipoly(Img);
end
'Ombre'
for i = 1:3
     close()
    maskOmbre{i}= roipoly(Img);
end

%Creation of the mask for every class
Plante = maskPlante {1} + maskPlante {2}+maskPlante {3} +maskPlante{4} + maskPlante{5};
Sol = maskSol {1} + maskSol {2} + maskSol {3};
Ombre = maskOmbre {1} +maskOmbre {2}+maskOmbre {3};

matPlante = strcat('Plante',plant,'.mat');
matSol = strcat('Sol',plant,'.mat');
matOmbre = strcat('Ombre',plant,'.mat');

save(matPlante,'Plante')
save(matSol,'Sol')
save(matOmbre,'Ombre')

load(matPlante)
load(matSol)
load(matOmbre)

%Creation of target and train matrixes
```

```
Target = zeros(15000,3);
for i = 1:ligne
 for j = 1:colonne
         if Plante(i,j) == 1
             l = l+1;
             for k = 1:3
             Train(l,k) = Img(i,j,k);
             end
              Target(l,1) = 1;
         end
         if Sol(i,j) == 1
             l = l+1;
             for k = 1:3
             Train(l,k) = Img(i,j,k);
             end
            Target(l,2) = 1;
         end
         if Ombre(i,j) == 1
             l = l+1;
             for k = 1:3
             Train(l,k) = Img(i,j,k);
             end
             Target(l,3) = 1;
         end
 end
end
save('l','l')
save('Train','Train')
save('Target','Target')

%Launching of the toolbox
nprtool

Image=zeros(8949072,3);
l=0;
for i = 1:ligne
 for j = 1:colonne
     l=l+1;
             for k = 1:3
             Image(l,k) = Img(i,j,k);
             end
 end
end

%Code generated by nprtool
Y =  myNeuralNetworkFunction(Image);
```

```
l=0;
for i = 1:ligne
 for j = 1:colonne
l=l+1;
             for k = 1:3
              Segm(i,j,k)= Y(l,k);
             end
 end
end

%Creation of the segmented image
l=0;
Segm = zeros(ligne,colonne);
for i = 1:ligne
    for j = 1:colonne
          l=l+1;
      if max(Y(l,:)) == Y(l,1)
        Segm(i,j) = 1;
      elseif max(Y(l,:)) == Y(l,2)
        Segm(i,j) = 0;
        elseif max(Y(l,:)) == Y(l,3)
        Segm(i,j) = 0;
      end
    end
end

%Elimination of the round aggregats
SE = strel('disk',3);
Segmbis = imopen(Segm,SE);

figure()
imshow(Segmbis)
```

Appendix 4: Script for variability between plots

```
%PlantCare calibration curve application
for i=1:5190

m1pc(i)=-1.228*10^(-5)*S1M(i)^3+0.01208*S1M(i)^2-3.98*S1M(i)+452.3;
m2pc(i)=-1.228*10^(-5)*S2M(i)^3+0.01208*S2M(i)^2-3.98*S2M(i)+452.3;
m3pc(i)=-1.228*10^(-5)*S3M(i)^3+0.01208*S3M(i)^2-3.98*S3M(i)+452.3;
m4pc(i)=-1.228*10^(-5)*S4M(i)^3+0.01208*S4M(i)^2-3.98*S4M(i)+452.3;
m5pc(i)=-1.228*10^(-5)*S5M(i)^3+0.01208*S5M(i)^2-3.98*S5M(i)+452.3;
```

```
m6pc(i)=-1.228*10^(-5)*S6M(i)^3+0.01208*S6M(i)^2-3.98*S6M(i)+452.3;
m7pc(i)=-1.228*10^(-5)*S7M(i)^3+0.01208*S7M(i)^2-3.98*S7M(i)+452.3;
m8pc(i)=-1.228*10^(-5)*S8M(i)^3+0.01208*S8M(i)^2-3.98*S8M(i)+452.3;
end
%Invalid data transformation
for i=1:5190
    if m1pc(i)<0
        m1pc(i)=0;
    else m1pc(i)=m1pc(i);
    end
    if m2pc(i)<0
        m2pc(i)=0;
    else m2pc(i)=m2pc(i);
    end
    if m3pc(i)<0
        m3pc(i)=0;
    else m3pc(i)=m3pc(i);
    end
    if m4pc(i)<0
        m4pc(i)=0;
    else m4pc(i)=m4pc(i);
    end
    if m5pc(i)<0
        m5pc(i)=0;
    else m5pc(i)=m5pc(i);
    end
     if m6pc(i)<0
        m6pc(i)=0;
    else m6pc(i)=m6pc(i);
     end
    if m7pc(i)<0
        m7pc(i)=0;
    else m7pc(i)=m7pc(i);
    end
      if m8pc(i)<0
        m8pc(i)=0;
    else m8pc(i)=m8pc(i);
    end
end
%Construction of SWC per plot
for i=1:5190
plot5m(i)=((m1pc(i)+m2pc(i)+m3pc(i)+m4pc(i))/4);
plot1m(i)=((m5pc(i)+m6pc(i)+m7pc(i)+m8pc(i))/4);
end
%Smoothing for temperature sensitivity
plot5m=smooth(plot5m,200);
```

```
plot1m=smooth(plot1m,200);

%Construction STD
for i=1:5190
if plot5m(i) < 2.5
    STDP(i)=plot5m(i) + 1.3896903;
    STDM(i)=plot5m(i)- 1.3896903;
elseif 2.5 < plot5m(i) < 7.5
    STDP(i)=plot5m(i) + 1.053;
    STDM(i)=plot5m(i) - 1.053;
elseif 7.5 < plot5m(i) < 12.5
    STDP(i)=plot5m(i) + 1.34325;
    STDM(i)=plot5m(i) - 1.34325;
elseif 12.5 < plot5m(i) < 17.5;
    STDP(i)=plot5m(i)+ 2.07211;
    STDM(i)=plot5m(i)- 2.07211;
elseif 17.5 <plot5m(i) <27.5
    STDP(i)=plot5m(i)+ 2.08806456;
    STDM(i)=plot5m(i)- 2.028806456;
else
    STDP(i)=plot5m(i)+ 1.07337;
    STDM(i)=plot5m(i)- 1.07337;
end
if plot1m(i) < 2.5
    STDP1(i)=plot1m(i) + 1.3896903;
    STDM1(i)=plot1m(i)- 1.3896903;
elseif 2.5 < plot1m(i) < 7.5
    STDP1(i)=plot1m(i) + 1.053;
    STDM1(i)=plot1m(i) - 1.053;
elseif 7.5 < plot1m(i) < 12.5
    STDP1(i)=plot1m(i) + 1.34325;
    STDM1(i)=plot1m(i) - 1.34325;
elseif 12.5 < plot1m(i) < 17.5;
    STDP1(i)=plot1m(i)+ 2.07211;
    STDM1(i)=plot1m(i)- 2.07211;
elseif 17.5 <plot1m(i) <27.5
    STDP1(i)=plot1m(i)+ 2.028806456;
    STDM1(i)=plot1m(i)- 2.028806456;
else
    STDP1(i)=plot1m(i)+ 1.07337;
    STDM1(i)=plot1m(i)- 1.07337;
end
end

tpc=datetime(DateTime,'InputFormat','dd.MM.yy_HH:mm:ss');
tprecip=datenum(tprecip);
```

```
%Plotting
fig = figure();
subplot(2,1,2)
left_color = [0 0 0];
right_color = [0 0 0];
set(fig,'defaultAxesColorOrder',[left_color; right_color]);
p1=plot(tpc,plot1m,'-r','LineWidth',2)
hold on
p2 = plot(tpc,plot5m,'-b','LineWidth',2)
p3 = plot(tpc,STDP,'--b',tpc,STDM,'--b',tpc,STDP1,'--r',tpc,STDM1,'--r')
xlim([datenum('23-May-2018 00:00:00') datenum('23-Jul-2018 10:04:25')])
ylim([0 35])
xlabel('Date')
ylabel('Volumetric soil water content [%]')
legend('C1','C5')
subplot(2,1,1)
p4=bar(tprecip,precip,0.2,'k')
ylim([0 1.5])
hold off
xlim([datenum('23-May-2018 00:00:00') datenum('23-Jul-2018 10:04:25')])
ylabel('Precipitations [mm]')
legend('Precipitations','Location','Best')
datetick('x','mmm dd','keeplimits','keepticks')
set(gca,'xtick',[])
```